REPORT NO. FAA-RD-81-41

DETECTION PERFORMANCE EVALUATION OF THE ASDE-3 USING FIXED FREQUENCY AND FREQUENCY-AGILE OPERATION

P.J. Bloom
G.J. Bishop
J.E. Kuhn

U.S.DEPARTMENT OF TRANSPORTATION
Transportation Systems Center
Cambridge MA 02142

MARCH 1981
FINAL REPORT

U.S.DEPARTMENT OF TRANSPORTATION
FEDERAL AVIATION ADMINISTRATION
Systems Research and Development Service
Washington DC 20590

Technical Report Documentation Page

1. Report No.	2. Government Accession No.	3. Recipient's Catalog No.
FAA-RD-81-41		

4. Title and Subtitle	5. Report Date
DETECTION PERFORMANCE EVALUATION OF THE ASDE-3 USING FIXED FREQUENCY AND FREQUENCY-AGILE OPERATION	April 1981
	6. Performing Organization Code: DOT/TSC/541
7. Author(s): P. Bloom, G. Bishop, J. Kuhn	8. Performing Organization Report No.: DOT-TSC-FAA-81-8
9. Performing Organization Name and Address: U.S. Department of Transportation, Transportation Systems Center, Cambridge MA 02142	10. Work Unit No. (TRAIS): FA121/R1135
	11. Contract or Grant No.
12. Sponsoring Agency Name and Address: U.S. Department of Transportation, Federal Aviation Administration, Systems Research & Development Service, Washington DC 20590	13. Type of Report and Period Covered: Jan 1980 - April 1980
	14. Sponsoring Agency Code: FA-ARD-100

15. Supplementary Notes

16. Abstract

The ASDE-3 Radar design has many features to enhance operational usefulness. The purpose of all these features is to provide a better airport surface surveillance display for the control tower cab. One of these features is the use of frequency agility, the transmission at a different frequency within a frequency band during each radar transmit time. The function of this feature is to improve the detection performance of the ASDE radar and thereby improve the quality of the information presented on the operational display. The use of frequency agility reduces image breakup of aircraft on the display and, in rainy weather, allows the display of ground traffic during much heavier precipitation than achievable with fixed frequency operation.

This report discusses the role of the ASDE in airport surface traffic control (ASTC), and the theory of frequency agility benefits, and gives the empirical results obtained during fiels experiments using the ASDE-3 engineering model test bed.

17. Key Words	18. Distribution Statement
ASDE; Airport Surface Detection Equipment; Frequency-Agile; Field Tests-ASDE-3	DOCUMENT IS AVAILABLE TO THE PUBLIC THROUGH THE NATIONAL TECHNICAL INFORMATION SERVICE, SPRINGFIELD, VIRGINIA 22161

19. Security Classif. (of this report)	20. Security Classif. (of this page)	21. No. of Pages	22. Price
Unclassified	Unclassified		

Form DOT F 1700.7 (8-72) Reproduction of completed page authorized

PREFACE

The Surveillance and Control Branch of the Transportation Systems Center under the program management of the Systems Research and Development Service ATC Automation Division (ARD-122) has concluded the ASDE-3 development program. The program included preliminary design review, critical design review, design, development, factory test, installation of the engineering model, engineering and operational evaluation and the technical data package documentation for product handoff to Airways Facility Service. This report is part of the technical data package, written to support Stage 4 (operational) spectrum approval. In particular, this report addresses the following spectrum approval items:

1. Provide test results demonstrating that a 10 kW, frequency agility ASDE radar system (versus a fixed frequency ASDE radar system) has improved detection performance, both in clear weather and rainy weather. This item is the major issue covered in the report.

2. Provide test results supporting the maximum spectrum occupancy required within the requested frequency band. This item is a subitem of 1, and is a minor report issue.

METRIC CONVERSION FACTORS

Approximate Conversions to Metric Measures

Symbol	When You Know	Multiply by	To Find	Symbol
	LENGTH			
in	inches	2.5	centimeters	cm
ft	feet	30	centimeters	cm
yd	yards	0.9	meters	m
mi	miles	1.6	kilometers	km
	AREA			
in^2	square inches	6.5	square centimeters	cm^2
ft^2	square feet	0.09	square meters	m^2
yd^2	square yards	0.8	square meters	m^2
mi^2	square miles	2.6	square kilometers	km^2
	acres	0.4	hectares	ha
	MASS (weight)			
oz	ounces	28	grams	g
lb	pounds	0.45	kilograms	kg
	short tons (2000 lb)	0.9	tonnes	t
	VOLUME			
tsp	teaspoons	5	milliliters	ml
Tbsp	tablespoons	15	milliliters	ml
fl oz	fluid ounces	30	milliliters	ml
c	cups	0.24	liters	l
pt	pints	0.47	liters	l
qt	quarts	0.95	liters	l
gal	gallons	3.8	liters	l
ft^3	cubic feet	0.03	cubic meters	m^3
yd^3	cubic yards	0.76	cubic meters	m^3
	TEMPERATURE (exact)			
°F	Fahrenheit temperature	5/9 (after subtracting 32)	Celsius temperature	°C

Approximate Conversions from Metric Measures

Symbol	When You Know	Multiply by	To Find	Symbol
	LENGTH			
mm	millimeters	0.04	inches	in
cm	centimeters	0.4	inches	in
m	meters	3.3	feet	ft
m	meters	1.1	yards	yd
km	kilometers	0.6	miles	mi
	AREA			
cm^2	square centimeters	0.16	square inches	in^2
m^2	square meters	1.2	square yards	yd^2
km^2	square kilometers	0.4	square miles	mi^2
ha	hectares (10,000 m^2)	2.5	acres	
	MASS (weight)			
g	grams	0.035	ounces	oz
kg	kilograms	2.2	pounds	lb
t	tonnes (1000 kg)	1.1	short tons	
	VOLUME			
ml	milliliters	0.03	fluid ounces	fl oz
l	liters	2.1	pints	pt
l	liters	1.06	quarts	qt
l	liters	0.26	gallons	gal
m^3	cubic meters	35	cubic feet	ft^3
m^3	cubic meters	1.3	cubic yards	yd^3
	TEMPERATURE (exact)			
°C	Celsius temperature	9/5 (then add 32)	Fahrenheit temperature	°F

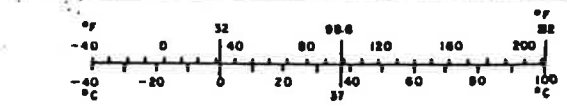

TABLE OF CONTENTS

LIST OF ILLUSTRATIONS

LIST OF ILLUSTRATIONS (CONT'D)

LIST OF ILLUSTRATIONS (CONT'D)

LIST OF TABLES

LIST OF SYMBOLS AND ABBREVIATIONS

ASDE	Airport Surface Detection Equipment
B	Receiver bandwidth
C	Speed of light
dB	Decibel power ratio of P_1 to P_2; 10 log (P_1/P_2) voltage ratio of V_1 to V_2; 20 log (V_1/V_2)
DAS	Data Acquisition Subsystem
dBm	Power level in decibels with reference to a power of one milliwatt.
dBic	Power level in decibels with reference to an isotropic circularly polarized radiator.
GA	General Aviation
GHz	10^9 Hertz
G_o	Peak antenna gain
$G(\theta)$	One way antenna elevation power pattern
$G(\phi)$	One way antenna azimuth power pattern
L	System Losses
L_p	Cancellation ratio
L_r	Rainfall attenuation loss
m	Meter
mm/hr	Millimeter per hour
MHz	10^6 Hertz
NF	Noise figure
ns	10^{-9} seconds
p-p	Peak-to-peak
P_c	Clutter power
P_d	Probability of detection

P_{fa}	Probability of false alarm
P_r	Power at receiver front end
P_t	Power transmitted at transmitter output
r	Slant range
RCS	Radar Cross-Section
S/C	Signal-to-clutter ratio
S/(N+C)	Signal to noise-plus-clutter ratio
STC	Sensitivity time control
n	Rainfall back scatter coefficient
λ	Wave length
σ	Radar cross-section
τ	Pulse width

1. INTRODUCTION

The ASDE-3 Radar design has many features to enhance operational usefulness. The purpose of all these features is to provide a better airport surface surveillance display for the control tower cab. One of these features is the use of frequency agility, the transmission at a different frequency within a frequency band during each radar transmit time. The function of this feature is to improve the detection performance of the ASDE radar and thereby improve the quality of the information presented on the operational display. The use of frequency agility reduces image breakup of aircraft on the display and, in rainy weather, allows the display of ground traffic during much heavier precipitation than achievable with fixed frequency operation.

This report discusses the role of the ASDE in airport surface traffic control (ASTC), and the theory of frequency agility benefits, and gives the empirical results obtained during field experiments using the ASDE-3 engineering model test bed.

2. SUMMARY

The results of the engineering evaluation of frequency agility presented in this report confirm that this technique significantly improves the operational effectiveness of the ASDE radar. Based on field data, frequency agility operation (versus fixed frequency operation) improves ASDE performance as follows:

Displayed target image breakup of large aircraft with aspect.	Reduced by 33%
Detection of small vehicles & aircraft with aspect change.	Improved by 4 to 6 dB; (power ratio from 2.5 to 4)
Rain weather detection of small aircraft & vehicles at ranges of less than 12,000 feet.	Improved by 9 dB; (power ratio of 8)

The rainfall performance can be improved further than the specified and demonstrated 16 mm/hour by the use of adaptive gain and threshold, operating with frequency agility. It is estimated, based on computer manipulation of field site rain data, that these techniques would allow clear display and detection of small targets in rainfall rates up to 50 mm/hour.

Based on field data, the performance benefits of frequency agility are improved by operating over a larger spectrum band width. The best performance was achieved operating over the maximum spectrum available, 360 MHz with a 70 MHz guard band at each end, (15.7 to 16.2 GHz; a 500 MHz band).

3. THE ROLE OF THE AIRPORT SURFACE DETECTION EQUIPMENT (ASDE) RADAR

Airport Surface Traffic Control (ASTC) is that system (people, procedures and equipment) which is concerned with the management of aircraft and vehicular traffic movement on an airport's runway and taxiway system. The ASTC system manages the flow of airport surface traffic to achieve (1) maximum safety and quality of service, (2) minimum aircraft delays to help reduce fuel use and air pollution, and (3) minimum costs for the users and the airport management agencies.

Airport Surface Traffic Control is exercised from the airport's control tower cab, located above the airport to provide good visual coverage of the airport's surface traffic movement areas. The ground controller, who controls traffic to and from the active runways as well as other taxiway traffic, uses visual observations through the tower cab windows to monitor the traffic. The local controller, who controls active runway traffic, uses visual observations and the Airport Surveillance Radar (ASR). The ASR provides the local controller final approach, initial climb and overall traffic pattern information on aircraft in the vicinity of the airport.

The role of ASDE is to provide ground surveillance information for the control tower during conditions of reduced visibility due to weather or darkness. The surveillance information provided by ASDE must be clear and accurate, and serve as a good replacement for the primary (visual) mode of ground surveillance. The resolution and imaging of traffic shown on the ASDE display should allow the controller to determine individual aircraft in queues and to determine aircraft type by size or shape.

4. FREQUENCY AGILITY OPERATION

Several steps were taken in the ASDE-3 design approach to improve the surveillance quality of the radar over the existing ASDE-2 and other ASDE type radars. Moving the frequency of ASDE from the ASDE-2 24GHz band to the 16 GHz band provided a significant improvement in rainfall penetration because of the more favorable attenuation and back scatter coefficients at the lower frequencies. The use of frequency agility improves target detection in rain clutter, improves target imaging with target aspect, and reduces the effect of ground multipath, (vertical lobing).

Frequency Agility Theoretical Background

A radar target is a complex arrangement of reflection scatters. The effective radar cross section of a target is dependent upon the target material, target geometry, the target aspect relative to the incident radar beam, the multipath effects and the illumination frequency.

The radar cross-section of a target has been a continuing subject for study and analysis. Models defined by Marcum for non-fluctuating targets and by Swerling for fluctuating targets allow targets to be classified as follows:

Case 0	Targets with near constant-valued radar cross sections.
Case 1 and 2: (Rayleigh Distribution)	Targets composed of a number of independent fluctuating reflectors of about equal echoing area.
	Case 1 targets fluctuate scan to scan.
	Case 2 targets fluctuate pulse to pulse.
Case 3 and 4; (Chi-square distribution)	Targets composed of one large reflector with a number of small reflectors.

Case 3 and 4 (Continued)

Case 3 targets fluctuate scan to scan.

Case 4 targets fluctuate pluse to pulse.

As with any model, the relationship between real targets and the model is never exact, but the above classifications have gained acceptance through empirical corroboration.

Detection of Aircraft and Vehicles: The aircraft and vehicle targets of interest for ASDE are generally of the type that fluctuate on a scan to scan basis. A scan to scan fluctuating target, Case 1 or Case 3, has limited decorrelation between pulses. During a single look at this type of target, (during an antenna beam width dwell time), the target return maintains a relatively constant cross section. The pulse-to-pulse integration gain in detection is similar to that achieved for a non-fluctuating target. These types of targets benefit from the integration of system noise. This characteristic of Case 1 and Case 3 targets is illustrated in Figure 4-1 which shows the theoretical detection performance curves for the five target models for a probability of detection of 0.9 and a probability of false alarm of 10^{-6}.

A pulse-to-pulse fluctuating target, Case 2 or Case 4, is characterized by decorrelation between pulses. During a single look at this type of target, the target returns change from pulse to pulse, providing independent samples of the radar cross section. Because the samples are independent, the dispersion around the mean of the radar cross section is decreased, thereby improving the pulse-to-pulse integration benefits. Figure 4-1 illustrates the pulse-to-pulse integration benefits for Case 2 and Case 4 target models. Note that these types of targets also benefit from the integration of system noise.

Frequency agility target detection benefits are a function of the radar system azimuth-range cell. For ASDE-3, with a pulse repetition rate of 20 kHz and an antenna rotation rate of once per second, there are 13 pulses during the 0.25 degree

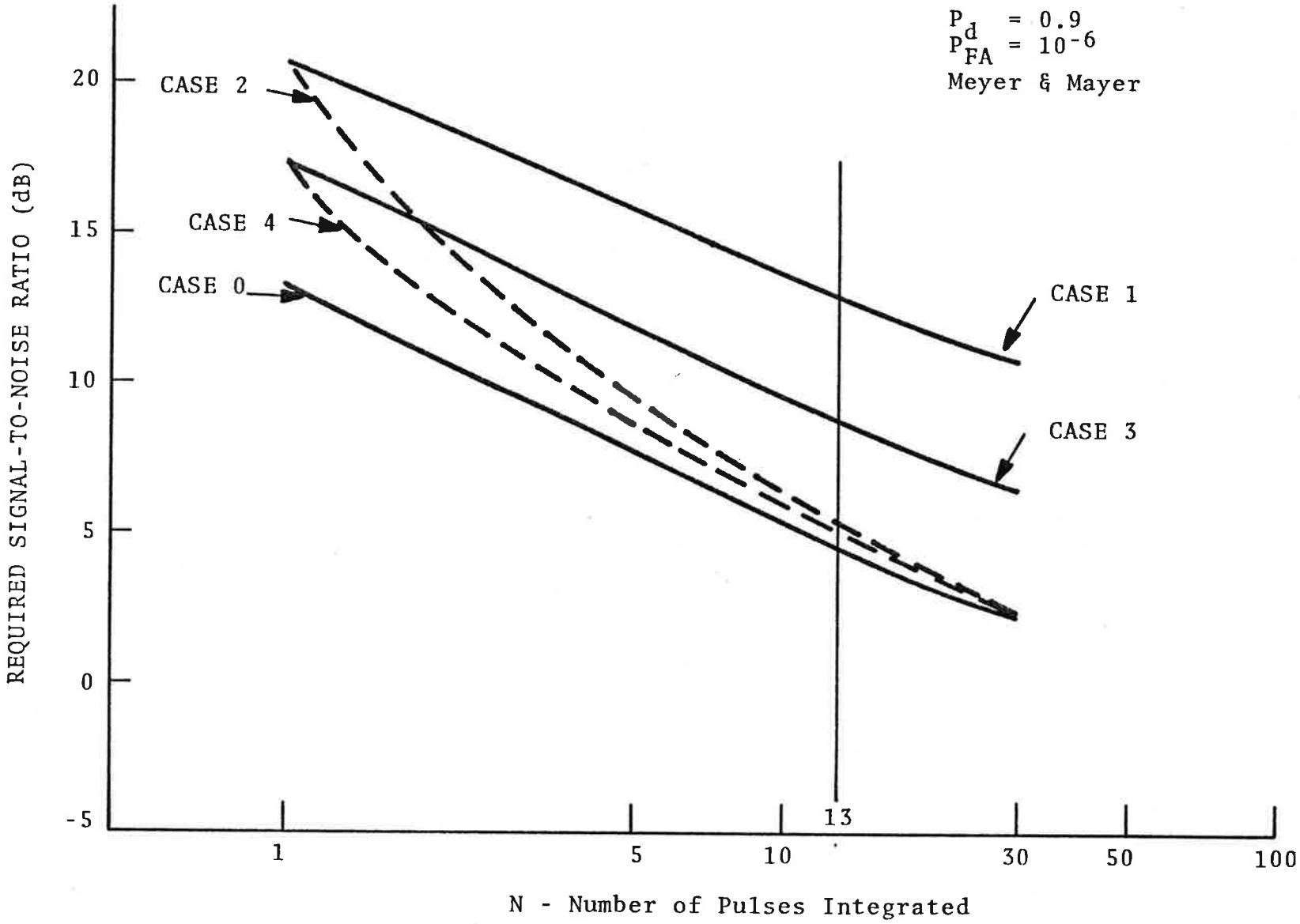

FIGURE 4-1. REQUIRED S/N VS PULSES INTEGRATED FOR CASES 0, 1, 2,3,and 4

azimuth beam width dwell time. Radar range (pulse width) resolution is approximately 18 feet. The integrator in the ASDE-3 system is the display, primarily the vidicon in the TV camera. The system integration benefits derived are a function of the display resolution cell and the integrator time constant.

Considering Case 1 and 3 targets, targets that fluctuate scan-to-scan, frequency agility provides decorrelated looks at these targets on each pulse, and effectively makes these targets look like pulse-to-pulse fluctuating targets. From Figure 4-1, changing the returns from a Case 1 target to a Case 2 target reduces the detection requirement by 7.7 dB for the same probability of detection and probability of false alarm. The Case 3 to Case 4 improvement is 3.8 dB.

Detection with target aspect change: The aspect of a complex target, (like an aircraft or vehicle), relative to the incident illumination beam, can greatly change the echo return. For ASDE, it is highly desirable to maintain returns from the same target near the same amplitude level in order to allow recognition of the target on the display by general shape, size or intensity. It is also highly desirable not to have breakup of larger targets, whereby an actual single target appears as two or more elements on the controllers display.

Several factors significantly influence the return seen from a rotating or moving aircraft on the airport surface; (1) the effective radar cross-section for the particular aspect angle, (2) the frequency of illumination, and (3) the vertical lobing effects.

As discussed previously, the return from a complex target, (a fluctuating target) will vary with the frequency of illumination. The variation in amplitude results from the phase relationship of the target's scatterers relative to the phase of the illumination frequency. This same phenomenon occurs if the target is rotated or moved in range or azimuth. The use of frequency agility smooths the echo returns from the fluctuating

target. This results in obtaining a better estimate of the target's radar cross section. Figure 4-2 illustrates this effect, showing that the dispersion of the amplitude return from the fluctuating target is reduced by frequency agility operation. The improvement in non-extended target detection for aspect, (rotation or changes in range or azimuth) is the same as discussed previously, (3.8 to 7.7 dB), depending upon the fluctuating target type, (type 3 or type 2).

Detection in the airport multipath environment: Another important target effect seen in the ASDE environment is caused by surface reflection multipath, (or vertical lobing). This effect is seen in returns from any target above the surface, small or extended targets; stationary, moving or rotating. This multipath effect results from the target being illuminated by competing signals, (the direct path from the antenna, and the ground reflected ray path), and from the target echo returning to the antenna over a direct and a ground reflected path.

Surface reflection multipath is a function of the target height above the ground, the surface reflectivity, the range of the target from the antenna, and the antenna's height above the surface. Figure 4-3 illustrates the vertical lobing geometry and provides the equations for the effects of vertical lobing on radar cross section. Notice that wave length is in the denominator of the phase (phi) equation. Thus, the use of frequency agility changes the net radar cross-section due to vertical lobing, from pulse-to-pulse, allowing a better estimate of mean echo strength, and this in turn improves target detection. The band over which the frequency can be changed is limited, and thus, (again looking at the phi equation), the effectiveness of frequency agility is range limited, with the most benefit derived at the shorter ranges. Frequency agility is predicated to have an effect in reducing vertical multipath out to a range of 6000 feet, depending upon the antenna tower height and other factors previously mentioned. At 500 feet, frequency agility was shown by test to reduce target cross-section dispersion by up to 8 dB.

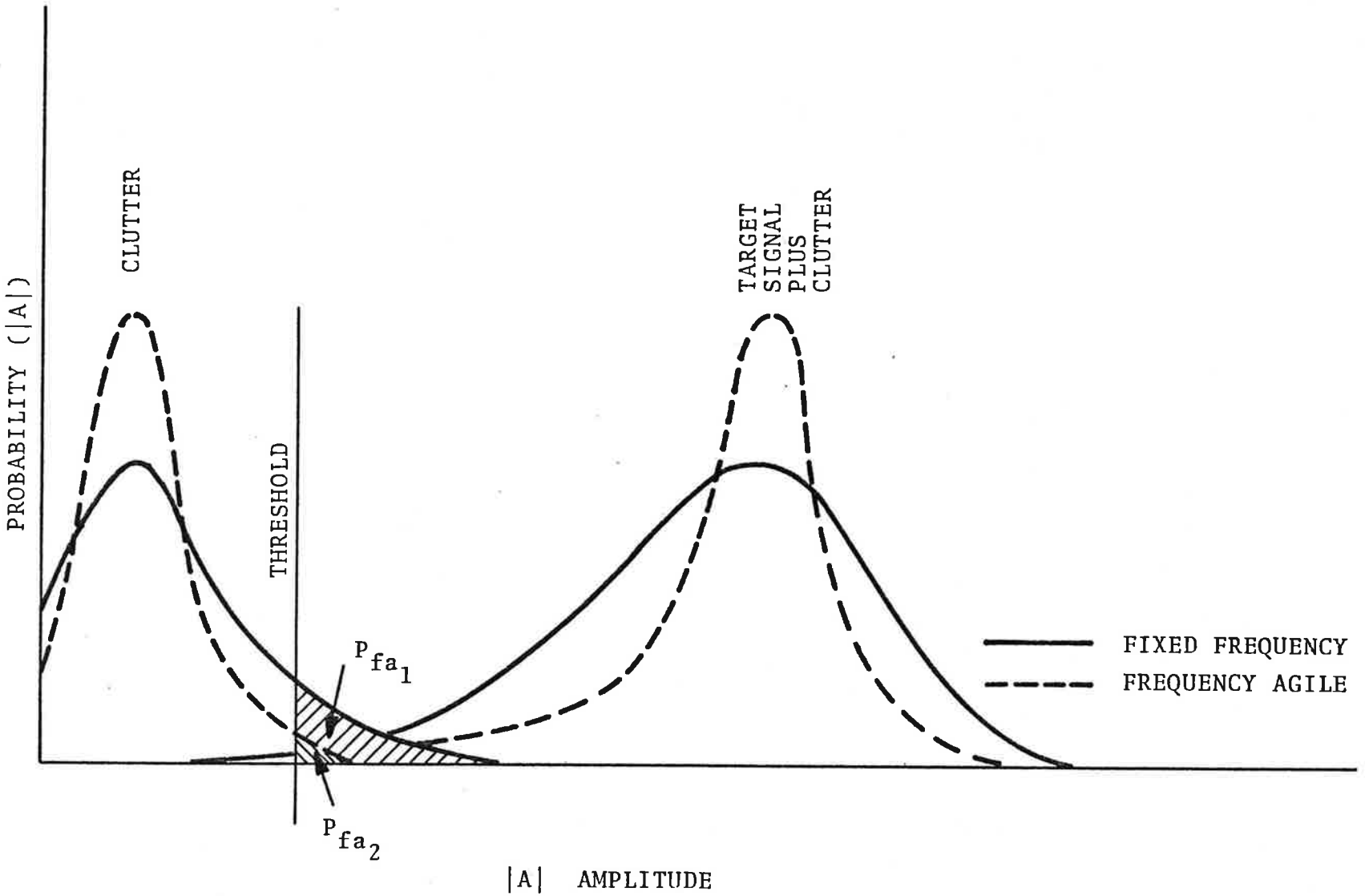

FIGURE 4-2. GRAPHICAL ILLUSTRATION OF TARGET AMPLITUDE DISTRIBUTION, THRESHOLD, & FALSE ALARM

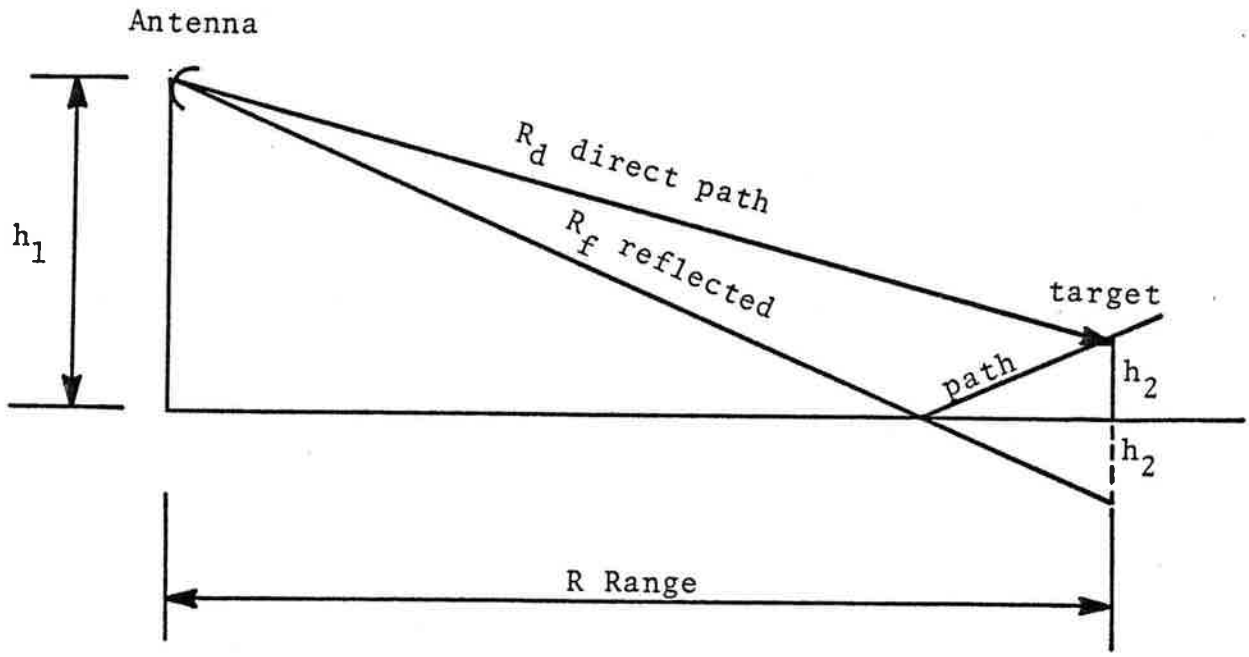

$$R_f = \left[(h_1+h_2)^2 + R^2 \right]^{1/2}$$

$$R_d = \left[(h_1-h_2)^2 + R^2 \right]^{1/2}$$

$\Delta R = R_f - R_d$

ϕ = phase difference between R_d and R_f path

$$\phi = \frac{2\pi}{\lambda} \Delta R$$

σ_e = effective radar cross section

σ_t = target radar cross section

ρ = ground reflection coefficient ($\rho \leq 1$)

$$\sigma_e = (1 + \rho^2 + 2(\rho \cos\phi))^2 \sigma_t$$

FIGURE 4-3. VERTICAL LOBING-EFFECTS ON RADAR CROSS-SECTION

Detection of rain: The clutter return from rain is from many individual scatterers of about the same size, and has an amplitude distribution that can be described as Rayleigh. At the pulse repetition rate used by ASDE, (Δt=50 microseconds), the scatterers within a radar resolution cell appear to be fixed during an azimuth beamwidth dwell time. Fluctuations, (changes in scatterers or the scatterers' positions), occur on a scan-to-scan basis. Typically temporal decorrelation for rain is approximately 10 milliseconds. Depending upon the arrangements of the rain drop scatterers, the clutter return can vary from a condition where the individual reflectors contribute to produce a maximum return, to a condition where the phase relationship between individual reflectors produces a minimum return. Thus, for any single frequency operation, the rain clutter signals can vary widely, requiring the threshold to be set at a level that allows for the large dispersion of the integrated clutter return. Setting the threshold at a higher level to achieve the desired false alarm rate reduces the probability of detecting targets. The use of frequency agility decorrelates the return from the rain clutter on a pulse-by-pulse basis because of the change with frequency of the relative phase between scatterers. Independent samples of the rain clutter echo strength are obtained, allowing a better estimate of the rain clutter mean echo strength by integration. For the same probability of false alarm, frequency agility operation allows a lower threshold to be set, and thus improves the probability of detecting targets. Figure 4-2 illustrates the effects of frequency agility in obtaining a better estimate of target and clutter amplitude and reducing false alarm rate for the same threshold. The solid lines in Figure 4-2 represent an illustration of the amplitude distribution for integrated rain clutter and target returns using fixed frequency. On a single scan, using fixed frequency, a particular value within the distribution would be returned to the radar during the azimuth beam width dwell time and the pulses integrated.

The dotted lines in Figure 4-2 represent an illustration of the amplitude distribution for integrated rain clutter and target returns using frequency agility. A better estimate of the rain clutter and target amplitude is obtained, as illustrated by the narrower distributions.

The cross-hatched lines in Figure 4-2 identify clutter amplitude above threshold, indicating the probability of a false alarm. As illustrated, the false alarm rate for fixed frequency is greater than for frequency-agile for the same threshold.

Rain clutter, when the rain is illuminated by frequency-agile transmissions, can be treated like system noise, acting in much the same manner as Marcum's analysis of a non-fluctuating target against a noise background. In both cases, each detected return within the integration cell limits is an independent sample and the distribution of the samples is Rayleigh. Consequently, the signal to clutter (S/C) improvement that may be theoretically achieved by integration using frequency agility is the same as that determined by Marcum for a non-fluctuating target against noise. For a 13-pulse integration, a probability of detection of 0.9 and a probability of false alarm of 10^{-6}, the theoretical S/C improvement using frequency agility in rain is 8.8 dB (refer to Figure 4-1; the difference between Case 0 at N equal to 1 and N equal to 13.) This is the improvement due to the effects of frequency agility on the rain clutter distribution.

The net target-to-clutter improvement has to consider the target characteristics. For a non-fluctuating target, Case 0, the improvement is the same as above, 8.8 dB. For a Case 1 target, the theoretical improvement is 8.8 dB plus 7.7 dB, or 16.5 dB. For the Case 3 type target the theoretical improvement is 8.8 dB plus 3.8 dB or 12.6 dB.

5. TEST AND EVALUATION RESULTS

The results of the ASDE-3 system testing at the FAA Technical Center (FAATC) are presented in this section. These tests include measurements on calibrated test reflectors and real targets. The real targets, (small aircraft, compact automobiles and large aircraft) were rotated in clear weather to study the effects of varying aspect on radar cross section. Calibrated target tests included the measurement of vertical multipath effects. Measurements of system performance were taken in rainfall by recording the radar returns from fixed reference reflectors and rain backscatter, and recording the rainfall rate readouts from rain gauges. All measurements were taken using both fixed frequency and frequency-agile modes of operation to obtain quantitative comparisons. The results of the tests are summarized in the following paragraphs.

a. Clear Weather Detection (Real Target Imaging)

Frequency agility (vs fixed frequency operation) improves the detection of small vehicles and aircraft whose return fluctuates with aspect change, by reducing the required signal-to-noise ratio by 4 to 6 dB. (See Section 5.2). For 90 percent probability of detection on the integrated target distribution the frequency agile benefit is 4 dB; and for 100 percent probability, the benefit is 6 dB. Peak-to-peak target fluctuations were reduced from 25 dB with fixed frequency to 10 dB with frequency agility.

Frequency agility benefits are increased by operating over a larger spectrum bandwidth. Operating over 360 MHz resulted in a 4 dB reduction in the required signal to noise ratio over operation at 180 MHZ. (See Section 5.2).

Tests conducted using large aircraft showed that target breakup with aspect was reduced by 33 percent using frequency agility. (See Section 5.3).

b. Clear Weather Detection (Vertical Multipath Effects)

Frequency agility (vs fixed frequency) reduced the effects of vertical multipath by 8 dB at the 500-foot range. (See Section 5.1). Frequency agility (vs fixed frequency) is predicted to reduce the effects of vertical multipath for ranges out to approximately 6000 feet.

c. Detection Performance in Rain (Fixed Reflector Measurements)

Frequency agile (vs fixed frequency) was demonstrated to improve detection of non-fluctuating targets in rain clutter by 5 dB. (See Section 5.4.) The theoretical benefit predicted is 8.8 dB. The improvement in rainfall detection for small, real (complex), fluctuating targets based on the rainfall and clear weather data is up to 9 dB for ranges of 12,000 feet or less. The theoretical benefit predicted is 12.6 dB. Frequency agility improvement in target detection performance is effective in regions of rain clutter predominence, as opposed to attenuation-limited regions. Frequency agility is, therefore, most effective at ranges within 12,000 ft.

d. Detection Performance in Rain (Frequency Agility Operation with Adaptive Gain and Threshold)

The benefits of frequency agility can best be realized using adaptive gain and thresholding. Quantitative values have not been determined for the improvements shown in qualitative pictorials produced by computer manipulation of gain and threshold, using recorded rain data. However, the qualitative pictorial results indicate that there is a substantial improvement in probability of detection and probability of false alarm. (See Section 5.5).

5.1 RADAR CROSS SECTION MEASUREMENTS

The objectives of these experiments were as follows:

a. Determine the radar cross section of test reflectors, aircraft and vehicles in the ASDE environment;

b. Determine the effects of vertical lobing on radar cross-section using fixed frequency and frequency agility operation;

c. Establish reference test reflectors for use in real (aircraft) target experiments and in rain test experiments.

5.1.1 Measurement of Calibrated Radar Reflectors

a. Test Reflector Description

Six small and two larger lens-type reflectors were used in system calibration. The reflectors are specially constructed to reflect circularly polarized radiation by use of a metal grid covering the lens. The lens is constructed of a closed-cell expanded polystyrene foam, backed by a reflective coating. The assembly is environmentally sealed by a plastic cap. Lens reflectors have broad acceptance angles ($\pm 45°$ in the case of the delivered samples). The reflectors had been measured on a radar cross-section range. Free space radar cross sections are nominally $1.5m^2$ for the small reflectors and $5m^2$ for the larger.

b. Vertical Lobing Measurement

To study the variation in radar return from the reflectors as a function of height above ground, the targets were systematically raised and lowered while the radar return was recorded by the Data Acquisition Subsystem (DAS) and plotted on-line (Figure 5.1-1). A remotely controllable motorized jack stand covered with Ecco-sorb was used to raise and lower the target to provide accurate and consistent results.

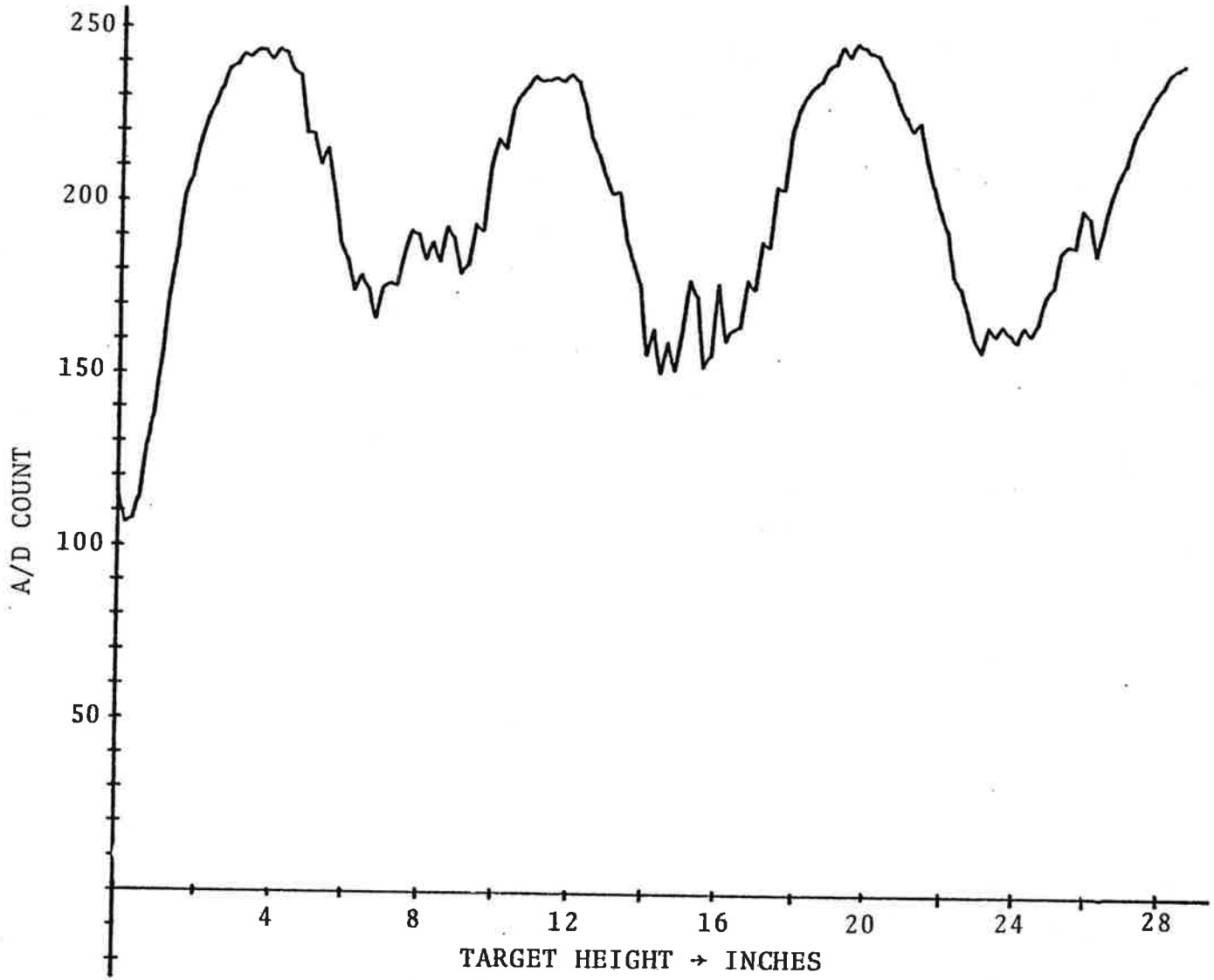

FIGURE 5.1-1. RADAR REFLECTOR RETURN VARIATION AS A FUNCTION OF HEIGHT ABOVE GROUND RUNWAY 17-35 (FIXED FREQUENCY)

As predicted by vertical lobing theory, radar returns from the targets are very sensitive to height above reflective terrain. The flat expanse of an airport provides a good reflective surface to support vertical multipath, and the broad acceptance angle of the lens reflectors readily receive from,and scatter energy back to, the ground. Table 5.1-1 shows the amplitude variation and the periodicity of the vertical lobing measured at four test ranges.

The substantial variation in measured radar cross-section (RCS) as the target is varied in height above ground (greater than the receiver dynamic range in some cases), reveals the difficulties some experimenters may have experienced in the past in making radar cross-section comparisons between free-space calibrated reflectors and aircraft and vehicle targets. A 30 dB variation in return from a $3m^2$ reflector can make it appear to be sized anywhere from $0.03m^2$ to $30m^2$. The technique using the jack stand proved effective and was used for all subsequent reference target data collection to obtain peak RCS values.

An optimum target height above ground was chosen for each test pad by finding the point where:

1. The target resides on a vertical lobing peak.
2. The target amplitude is least sensitive to frequency changes. These two heights, in general, occur at the same point.

c. Frequency Agility Effects on Vertical Multipath

The first quantitative indication of the effects of frequency agility on target returns was observed during these vertical lobing tests. As seen in Figure 5.1-2 the target periodicity at pad 1 is about 2" of vertical travel from null-to-null. This lobing pattern maintains the same periodic behavior for each of the fixed frequencies with the entire pattern shifted up or down, depending upon the particular fixed frequency used. For each test run 5 pulses were averaged. When frequency agility was used, the vertical lobing pattern nearly disappeared for pad 1 (Figure 5.1-3), going from 10 dB p-p to 2 dB p-p.

TABLE 5.1-1. RADAR TEST REFLECTOR VERTICAL LOBING MEASUREMENTS (FIXED FREQUENCY)

PAD	RANGE	PEAK-TO-PEAK AMPLITUDE	MEASURED PERIODICITY (null-to-null)
1	500 ft	8-10 dB	2"
Run-way 17/35	2100 ft	12 dB	8.2"
2	4900 ft	20 to 28 dB	15 to 23"
3	8500 ft	28 dB	30"

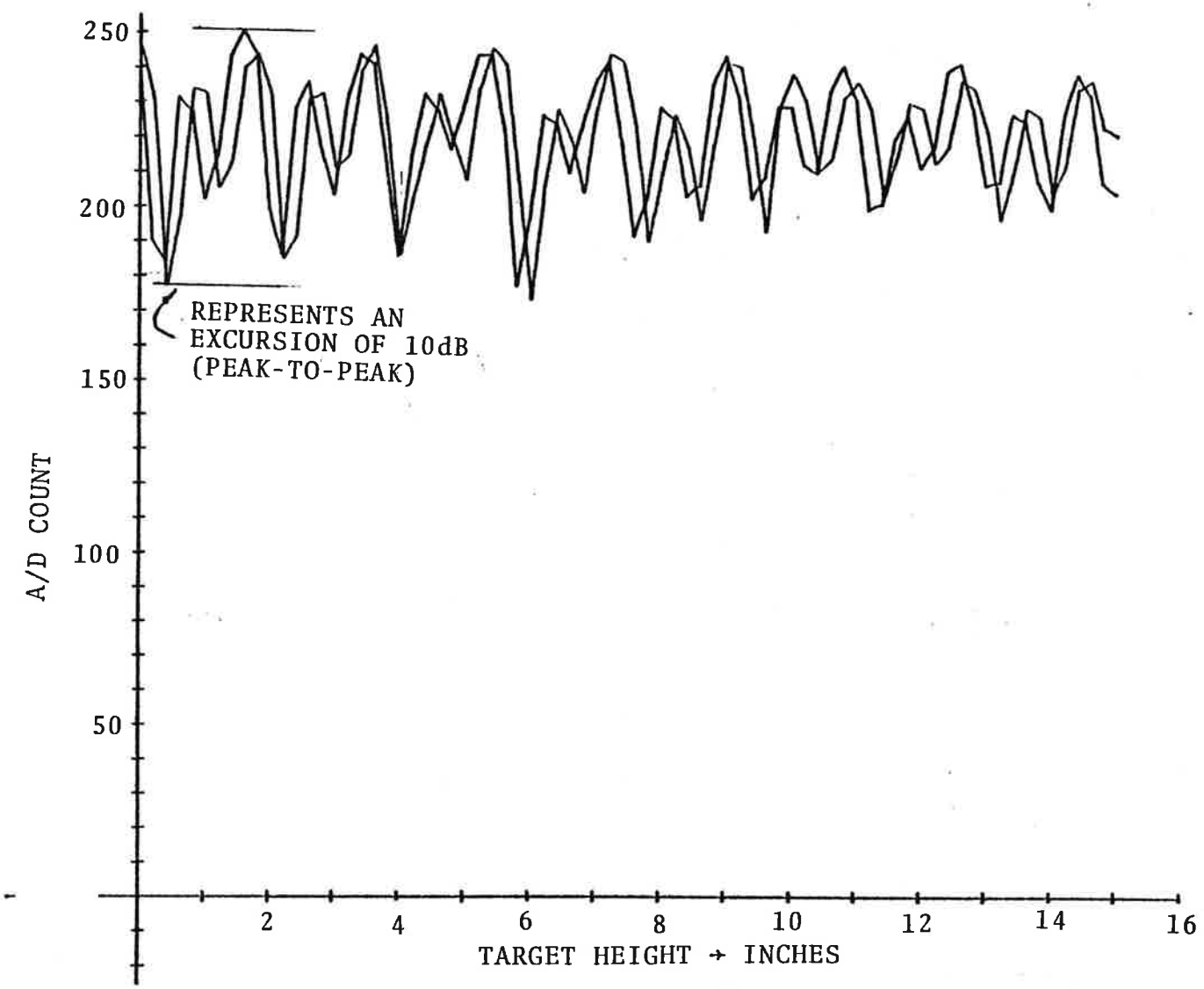

FIGURE 5.1-2. REFLECTOR RETURN VARIATION AS A FUNCTION OF HEIGHT ABOVE GROUND - PAD 1 (FIXED FREQUENCY)

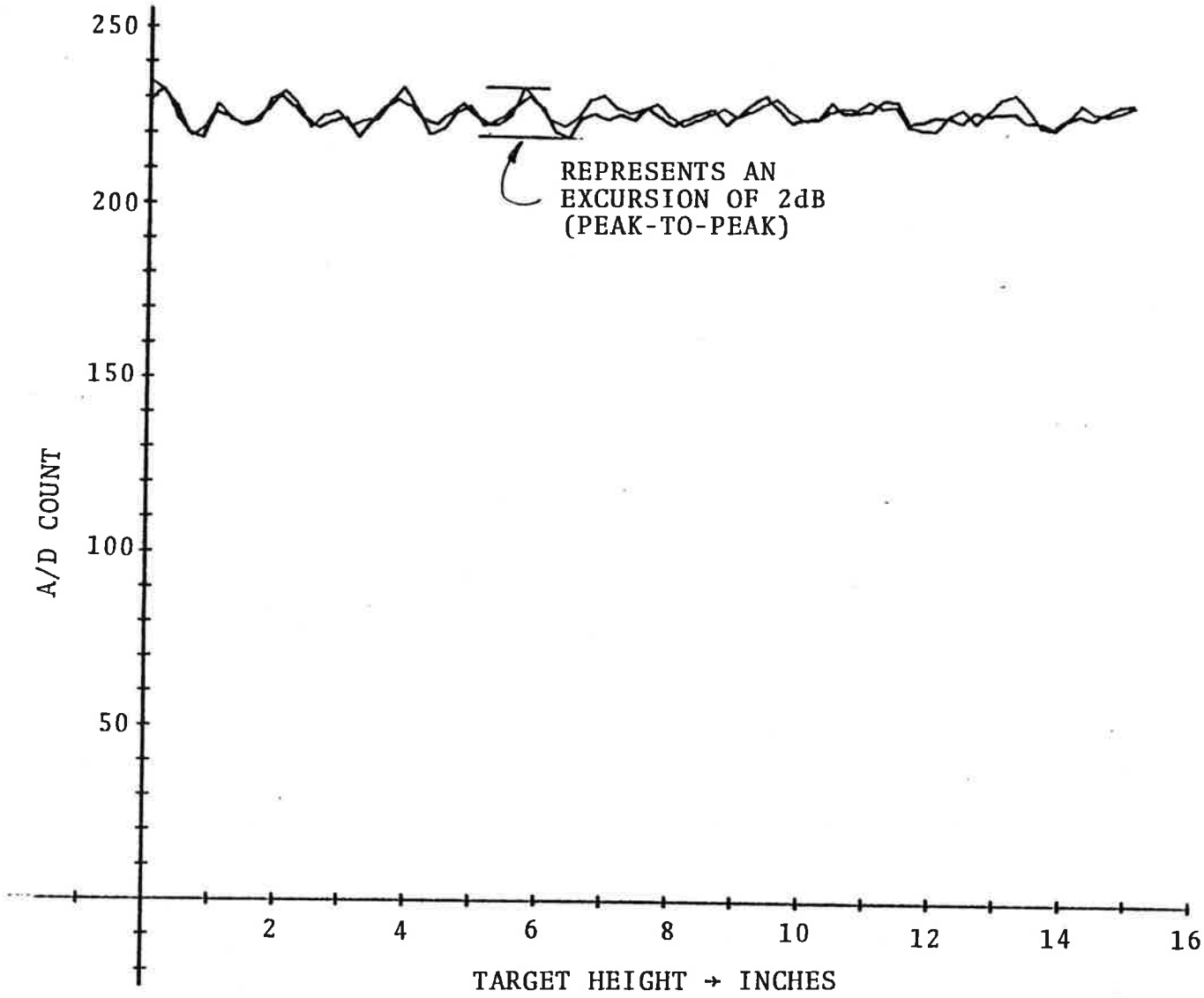

FIGURE 5.1-3. RADAR REFLECTOR RETURN VS HEIGHT ABOVE GROUND: 5-PULSE AVERAGE USING FREQUENCY AGILITY (PAD 1)

The smoothing effect of frequency agility on target amplitude fluctuations due to phase effects is predicted by theory. The amount of smoothing where phase effects are due to vertical lobing depends upon target range. Relatively little frequency-agile smoothing of the target return was found at pad 3, some at pad 2 (see Figure 5.1-4) and nearly total smoothing at pad 1. The smoothing effect is a function of ASDE tower height as well as range, with the effect seen over greater ranges for the higher towers and for greater target heights.

These target tests were an interesting precursor to the imaging tests conducted subsequently. As a result of all these tests, it was found:

1. The frequency sensitivity of a simple point target above reflective terrain (the airport surface) is of complex nature, but readily understood by theory.

2. Meaningful radar cross-section comparisons must be done by using the above described vertical travel test method.

3. The sensitivity of a real (i.e., aircraft or vehicle) target to fading will also be a function of height above ground and range from the ASDE, as well as target aspect. The period of the vertical lobing cycles becomes longer at greater ranges from the radar and as target height is reduced.

4. The ability to smooth returns from targets, which vary in aspect, by use of frequency agility depends upon the radial separation of the phase centers of the scattering centers primarily responsible for the radar return within a given range resolution cell. The farther apart these scattering centers are, the more the resultant return is affected by changing frequency. The consequence of this was seen in the measurements of small vehicle RCS.

d. Selection of Rain Data Reference Reflectors

Initially the vertical lobing measurements were all conducted using the larger ($5m^2$) reflectors. It was decided to use the

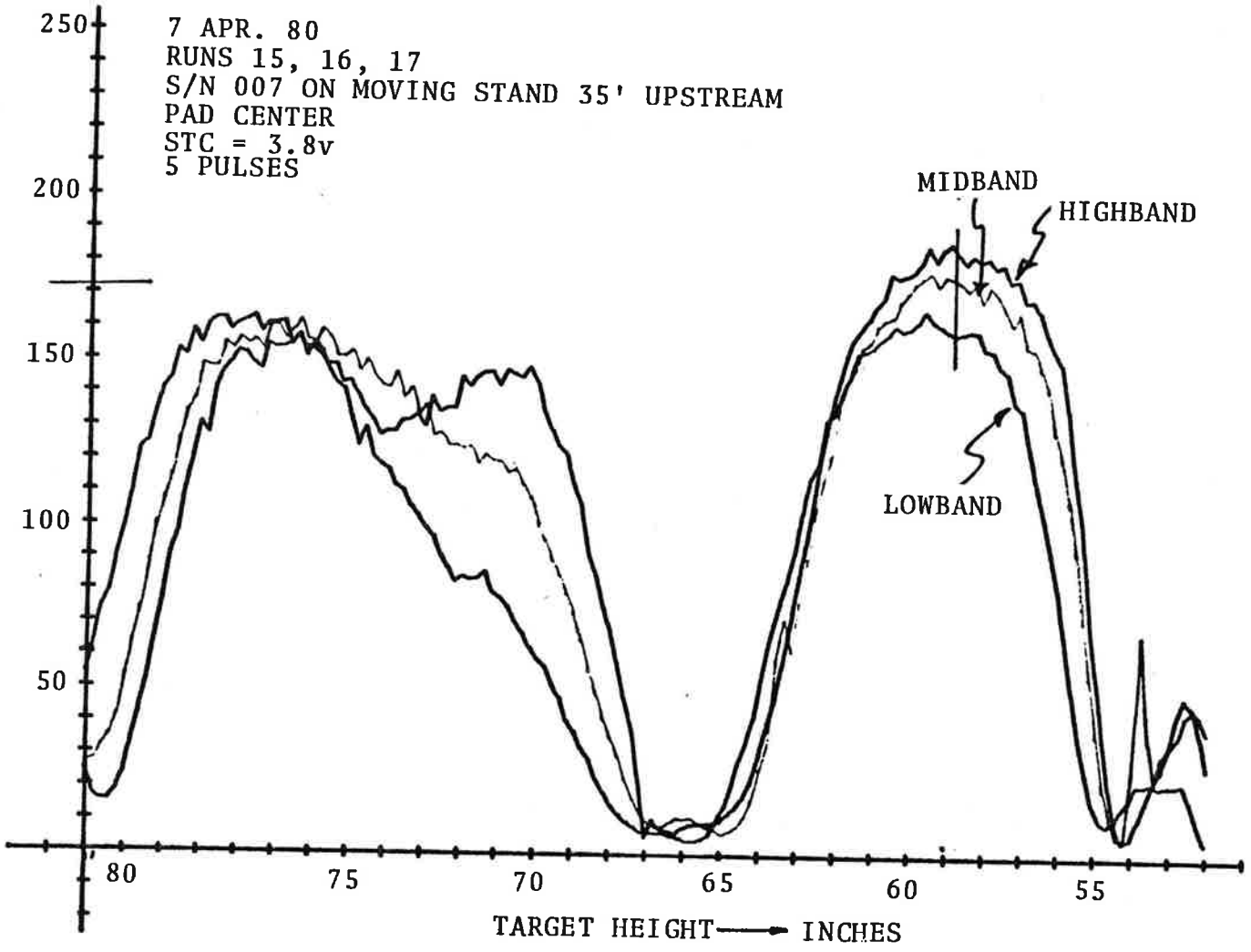

FIGURE 5.1-4. RADAR REFLECTOR VARIATION AS A FUNCTION OF HEIGHT ABOVE GROUND - PAD 2 SHOWING FREQUENCY EFFECTS

small ($1.5m^2$) reflectors at all pad locations to prevent receiver saturation during the high gain conditions required for rain data collection. However, when the smaller reflectors were substituted, considerable variation in reflected signal was observed between individual reflectors. Table 5.1-2 lists the results of signal return measurements for the lens reflectors tested at pad 2 and 3 locations. Two of the small reflectors (S/N 007 and 010) appeared significantly stronger than the other four. A 7 dB difference between the mean of the group of weaker reflectors and the two stronger $1.5m^2$ reflectors was measured. Measurement error for the particular comparison was held to a minimum because the data for all six reflectors was taken in a 4-hour period on a clear day with each reflector individually raised and lowered on the Eccosorb covered stand. The standard deviation of measurement error is estimated to be within 2 dB for such direct comparisons.

As a result of a 7 dB discrepancy, the small lens reflectors were not used for the rain data target comparison, and were returned to the contractor for diagnosis. The small sheet metal mounting bracket for the $1.5m^2$ lens reflectors provided a time and frequency-stable radar cross section on the order of 10 dB smaller than the two "good" $1.5m^2$ lens reflectors. The bracket essentially forms a dihedral corner reflector which returns circularly polarized radiation. The RCS computed for reflectors was $0.4m^2$. The bracket reflectors were chosen for use on all three pads as the rain data collection reference because of their identical construction, small RCS and stability with time and frequency.

e. Comparisons of Radar Cross Section Measurements to Theory:

The results of radar cross-section measurements for the brackets, $1.5m^2$ and $5m^2$ reflectors are shown on Figures 5.1-5 and 5.1-6, plotted on the theoretical line for their computed or measured RCS and compared to theoretical for the system at pads 2 and 3. All data points represent the reflectors at optimum heights (vertical lobing peak) by means of the vertical travel

TABLE 5.1-2. TEST REFLECTOR RADAR RETURN LEVELS

Pad 2 (4846 ft range)

SMALL LENS (1.5m^2 Free space)	AVERAGE RETURN POWER
S/N 007	-45.8 dBm
S/N 010	-45.7 "
S/N 008	-53.3 "
S/N 009	-55.3 "
S/N 011	-52.4 "
S/N 012	-52.1 "

7.4 dB difference

LARGE LENS (5m^2 Free space)	
S/N 066,067	-37.7 dBm

Pad 3 (8504 ft range)

LARGE LENS (5m^{2}free space)	
S/N 066,067	-46.2 dBm

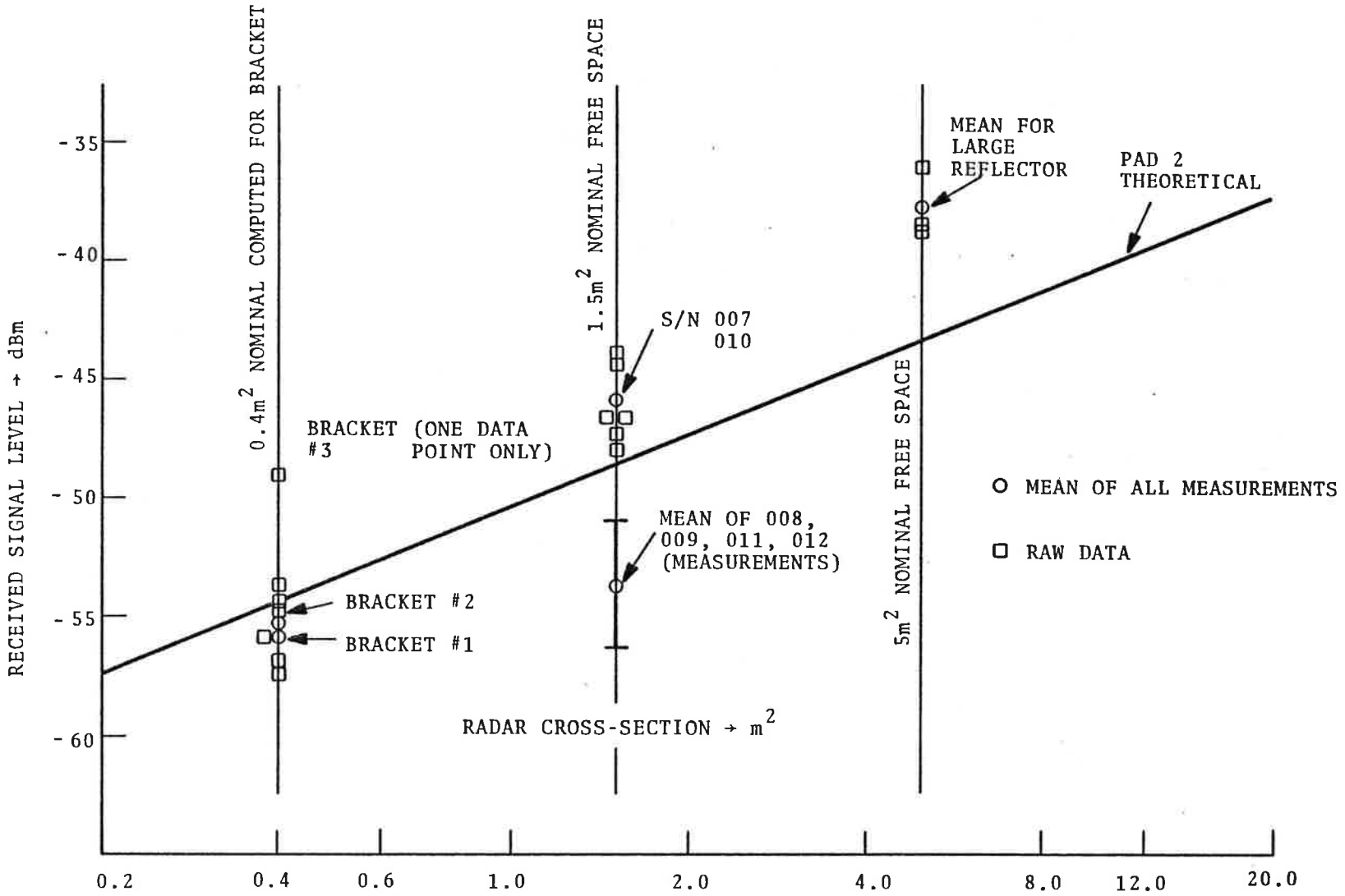

FIGURE 5.1-5. TEST REFLECTOR RADAR CROSS SECTIONS MEASURED AT VERTICAL LOBING PEAK-PAD 2

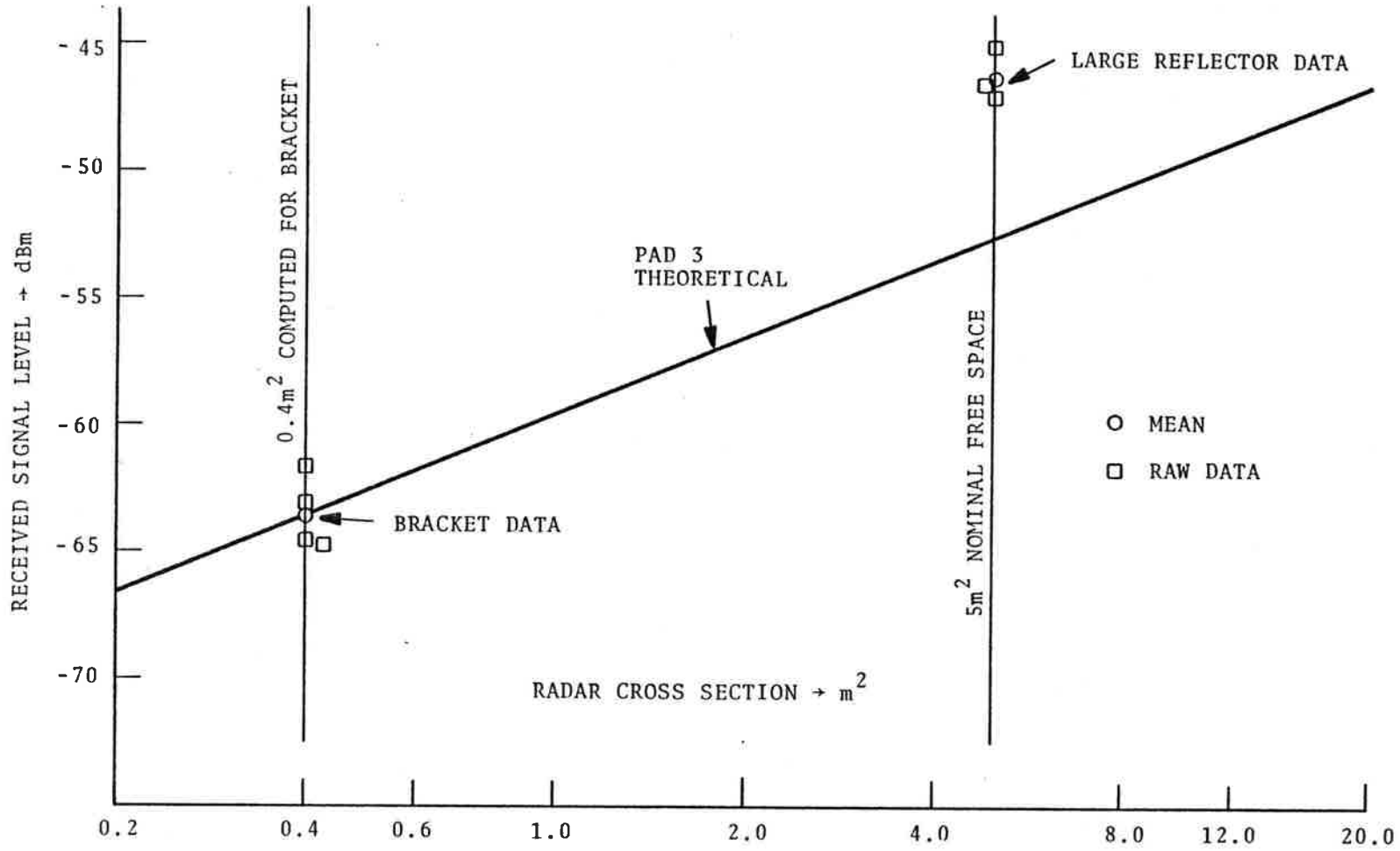

FIGURE 5.1-6. TEST REFLECTOR RADAR CROSS SECTIONS MEASURED AT VERTICAL LOBING PEAK-PAD 3

tests described earlier. Table 5.1-3 lists the radar equation parameter values used in computing the theoretical return values.

After considerable study of the target return data from the standard reflectors, the following observations were made:

1. Absolute calibration of the radar is a difficult task. Even when careful control of the vertical multipath environment is exercised, considerable target return deviation is seen from theoretical flat earth vertical lobing predictions. From the data collected it is difficult to tell whether the large reflectors are 6 dB high due to vertical lobing enhancement (entirely possible) or some other systematic reason. The mean returns from the two "good" $1.5m^2$ reflectors lie 3 dB above the theoretical curve, in the right direction for vertical lobing enhancement. The small bracket returns lie right on the theoretical curve for both pad 2 and 3 plots suggesting that their free space RCS (σ) is not as large as the $0.4m^2$ computed using the standard dihedral reflector equation

$$\sigma = \frac{8\pi a^2 b^2}{\lambda^2}$$ where a and b

are the dimensions of a single side. The data strongly suggests that the peak RCS for a non-directive reflector above smooth airport terrain is 3 to 6 dB higher than for free space.

2. Relative radar cross-section measurements are achievable with good accuracy. Each raw data point on the figures represents an independent sample in time or target location. The standard deviation of same-day comparison measurements largely comes from uncertainty in the receiver calibration curve, short-term system drift and variation in the peak vertical lobing enhancement from target-to-target due to subtle differences in target

TABLE 5.1-3. ASDE-3 SYSTEM PARAMETERS USED IN RADAR EQUATION COMPUTATIONS

P_r	Power received at rf amplifier	solve for
P_t	Power transmitted measured at output of the circulator	+ 68 dBm
L	System losses, input to pedestal	13.5 dB
λ	Wavelength at 16 GHz	0.06152 feet
δ	Radar cross section	variable (m^2)
r	Slant range, antenna to	
	Pad 2	4846 feet
	Pad 3	8508 feet
$G(\theta_2)$	Antenna gain at Pad 2	44.6 dBic
$G(\theta_3)$	Antenna gain at Pad 3	45 dBic

$$P_r = \frac{P_T \lambda^2 L G^2 (\theta) \delta}{(4\pi)^3 r^4}$$

scattering patterns. The one-sigma error is within 2 dB for the composite, consistent with the clustering of the raw data points on the figures.

Two comparisons made which support the validity of the ASDE as a radar measurement tool are:

1. RCS measurement of the large ($5m^2$) and small "good" ($1.5m^2$) lens reflectors at pad 2 at optimum heights above ground made within a 20 minute period March 20, 1980 showed a 5.7 dB difference in return level between the two. 10 log (5/1.5)=5.2 dB theoretical.

2. The mean of all measurements between the large lens reflectors and the two "good" small lenses is 8 dB, which includes data over a period of 5 months introducing the effects of long-term drift and additional receiver calibration uncertainty.

5.1.2 Measurement of Real Targets

Several real targets of operational interest were rotated through 180° (360° in some cases) to study fluctuations in radar cross section with changing aspect. Targets tested ranged in size from a compact car to a large aircraft. A detailed presentation of the results appears in Section 5.2 and 5.3. A summary of the results of the measurements is shown in Table 5.1-4. The values shown represent the peak RCS for each target as recorded by the DAS and do not include the effect of integration across the ASDE display resolution element. See Figure 5.1-7 for an example of the DAS data window showing an extended target with the location of the peak return value indicated. All measurements discussed in this section were taken using fixed frequency data.

Although the large aircraft exhibit relatively low peak RCS values for certain aspects (3 to $5m^2$ for the 727 and 880), detectability is significantly greater on the display than for a point target of the same RCS. It is interesting to note that the relatively low maximum RCS for the large aircraft ($\sim 100m^2$) is not significantly higher than that of the Cherokee 180. The Cherokee

TABLE 5.1-4. VARIATION IN THE PEAK RADAR CROSS SECTION AS THE TARGET IS ROTATED 180°

TARGET	RADAR CROSS SECTION		
	MINIMUM IN THE 180° ROTATION	MEAN FOR THE 180° ROTATION	MAXIMUM IN THE 180° ROTATION
*Cherokee 180	$0.3m^2$	$5m^2$	$100m^2$
Compact Car	$0.2m^2$	$1.6m^2$	$10m^2$
727	$3m^2$	$6m^2$	$126m^2$
880	$5m^2$	$22m^2$	$158m^2$

Values represent the peak RCS value (five-pulse average, fixed frequency operation) selected from each window as the target was rotated 180°, display integration not considered. All values from data taken with fixed frequency operation. Cherokee data was sampled every 10° of rotation, compact car data sampled every 20° of rotation.

*Reference $5m^2$ reflector visible in data window, reference reflector on vertical lobing peak.

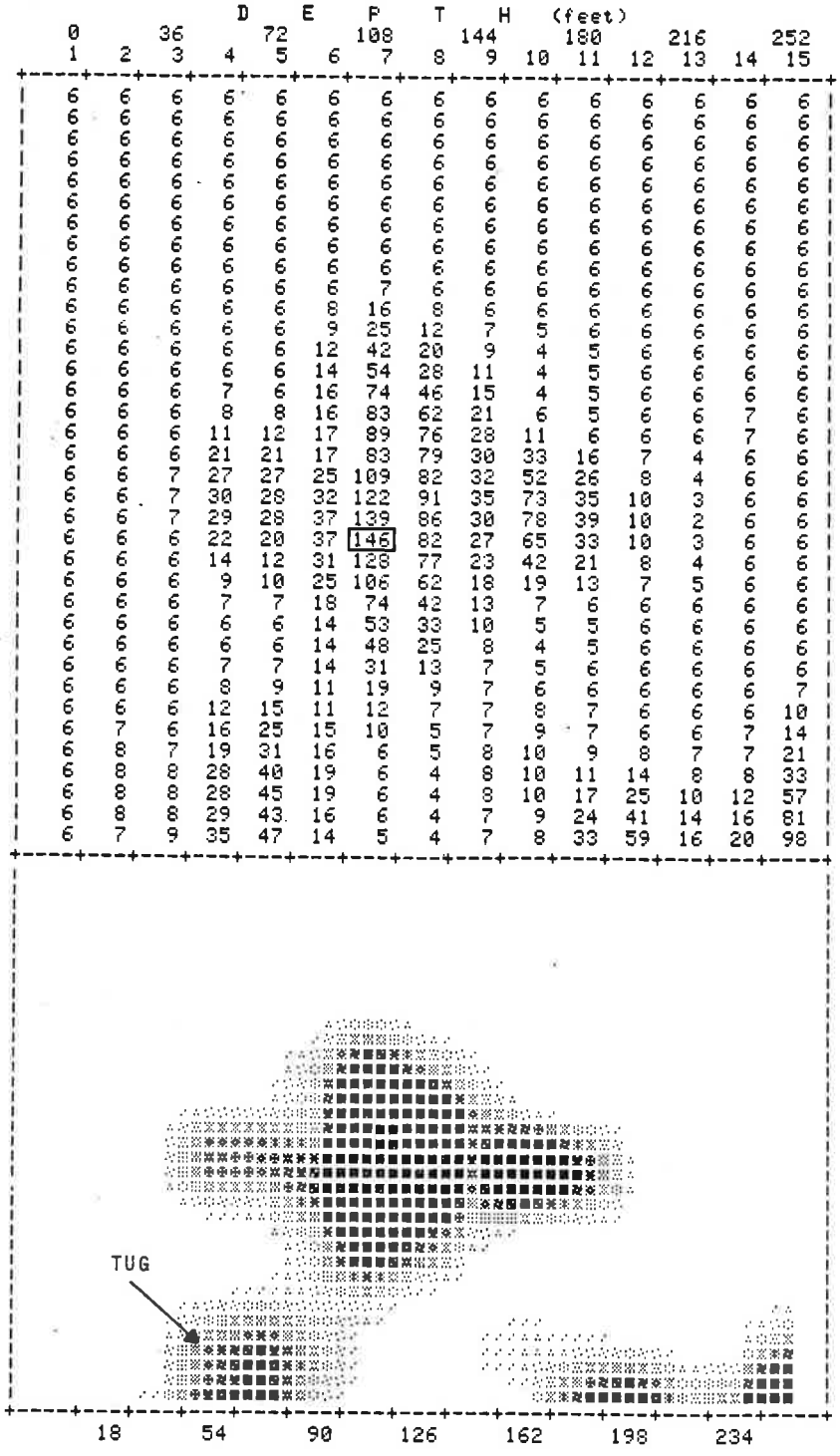

FIGURE 5.1-7. DAS RAW DATA WINDOW SHOWING LOCATION OF TARGET PEAK: CONVAIR 880

RCS value represents the summation of target power for the entire aircraft which lies within the antenna 3 dB beamwidth and the radar pulse width. At broadside, where the peak value was seen, the flat surfaces of the Cherokee (tail and slab fuselage) provide a very good return. The large aircraft, however, are resolved into several elements by the azimuth beam and radar pulse. The number or intensity of radar scatterers within a single resolution element are not necessarily greater than those seen by the radar looking at the small aircraft. If an entire 727 were integrated into a whole, then it would have a much larger peak RCS than the small aircraft. Also, a large aircraft at much longer ranges than available would have a larger RCS because more scatterers are integrated within the radar pulse volume, due to the increase in area intercepted by the beam at the greater range.

The peak-to-peak fluctuation for the small aircraft is an order of magnitude worse than for the large aircraft. The coarse (macro) fluctuation of the small car* is not as severe as the Cherokee because the car does not have the distinctive broadside peak characteristic of the aircraft. Section 5.2 discusses and presents plots of fine grained ($\sim$2°) RCS structure for the car, and shows the Cherokee coarse structure (10° increments) with the broadside peak evident.

For the small aircraft and automobile, the very small RCS values happen a small percentage of the time. The RCS value of interest is that which will give detection a specified percentage of the time. The effect of fluctuating targets on system performance is discussed in Section 5.6.

5.1.3 Section Summary

1. Peak RCS for a non-directive reflector above smooth airport terrain is 3 to 6 dB greater than that for free space due vertical lobing effects.

*Minimum to maximum data for the car shown in Table 5.1-4 based on 20° sampling from fine grained (2°) rotation data.

2. Meaningful RCS comparisons between calibrated and real targets (e.g., aircraft, vehicles, etc.) must be done by systematic vertical lobing tests using the reference reflector on an elevation stand. Otherwise, vertical lobing effects can lead to totally erroneous conclusions, in error by as much as 30 dB when the reference target is near a multipath null.

3. Frequency agility reduces the fluctuation in the multiple pulse-averaged returns from a point target in a vertical lobing environment. The smoothing effect is a function of target range and target height above ground.

4. Peak-to-peak fluctuation in the peak RCS for the smallest aircraft target (GA aircraft) is an order of magnitude greater than for the large aircraft.

5. The minimum RCS for macro-scale data (10° to 20° sampling) for both the small aircraft and the compact car are about $0.3m^2$. (See Table 5.1-4).

6. The small aircraft exhibited a very large RCS peak at broadside aspect (90°) estimated at $100m^2$, not representative of the majority of the remaining aspects. The small auto did not evidence the same characteristic.

7. The minimum peak RCS for the large aircraft was $3m^2$ for the 727. This does not represent impaired detectability, however, as measurements were taken with the aircraft resolved into several cells by the narrow ASDE beamwidth and pulse.

5.2 SMALL REAL TARGET DETECTION PERFORMANCE (CLEAR WEATHER)

5.2.1 Compact Automobile Detection

Ever since the ASDE-3 was installed at FAATC, considerable qualitative observation of the display was made as project vehicles were driven to and from the various test pads. The general impression was that an automobile was a readily discernible but highly variable target. An early such "experiment" involved the display observer counting missed scans while a rental car was driven on the perimeter road near pad 3, about 8000 ft in range. The target would disappear several times along the 1/2 mile route when operating the ASDE-3 on fixed frequency. The auto was missed for only one scan for the same route when frequency agility was used.

To quantitatively measure the ability of the ASDE-3 to detect small vehicles, a compact automobile was slowly driven in a small circle on taxiway K, about 7500 ft in range (1.25nm.) from the radar. The DAS recorded scan-by-scan signal returns. Two significant results were obtained:

a. A small vehicle whose dimensions fall within the antenna beam width is indeed a complex target. Phase effects cause the net radar cross-section to fluctuate wildly with very small changes in target aspect. Peak-to-peak fluctuations of 25 dB were measured for fixed frequency operation.

b. Pulse-to-pulse frequency agility reduces the effect of the scan-to-scan fluctuation by 15 dB providing a solid detectability improvement.

The Experiment

The automobile was driven in a circle, presenting a slowly changing aspect to the radar for a full 360°. Data was taken while the rotodome was scanning normally at 1 revolution per second (60 rpm). Two hundered scans of data were digitally

recorded making the average aspect change 1.8° per scan. The circle was repeated for a total of six different frequency patterns; two at fixed frequency and four frequency-agile patterns. See Table 5.2-1 for the frequency patterns used.

Data Reduction

The per-pulse detected video data in A/D counts was converted to received power referenced to the receiver input. For each scan radar returns from the entire target were integrated. The resulting single scan integrated values were plotted vs scan. Scan number is proportional to aspect angle, with 0 equal to head-on and scan 200 representing the completion of the full circle, returning to head-on.

Data Analysis

The fine grained fluctuation seen in Figure 5.2-1 (25 dB peak-to-peak) is caused by the complex summation of the individual scatterers which make up the automobile as a radar target. Minor aspect changes (less than 2°) drastically alter the phase sensitive sum of the collection of scatterers. The data shows the nulls appear frequently for fixed-frequency, considerably impairing target detectability. Figure 5.2-2 shows the fluctuation for frequency agility. Peak-to-peak fluctuation is reduced by 15 dB. A more meaningful measure of the radar detection performance is shown in Figure 5.2-3. Cumulative probability of detection (P_d) is shown for fixed and for agile operation. Detectability is the percent of total 200 scans appearing above a given threshold power level. The sharp-kneed characteristic of frequency agility clearly contrasts to the slowly changing detection curve for non-agility. For a P_d of 100%, the performance improvement for frequency agility is 6 dB. For a P_d of 90%, the benefit drops to 4 dB. Table 5.2-2 compares each frequency pattern detection performance to fixed frequency. A measurable benefit is observed when using larger spectrum widths for frequency agile operation, with 360 MHz being 4 dB better than 180 MHz at the 100% detection point. The benefit at the 90th percentile point is less.

TABLE 5.2-1 FREQUENCY PATTERNS FOR COMPACT CAR

PATTERN	BAND OCCUPIED*	
1	360 MHz	13 steps, 30 MHz each
4	240 MHz	9 steps, 30 MHz each
7	180 MHz	7 steps, 30 MHz each
12	180 MHz	13 steps, 15 MHz each
18	-------	Fixed Frequency-mid
19	-------	Fixed Frequency-high

*CENTER FREQUENCY-TO-CENTER FREQUENCY

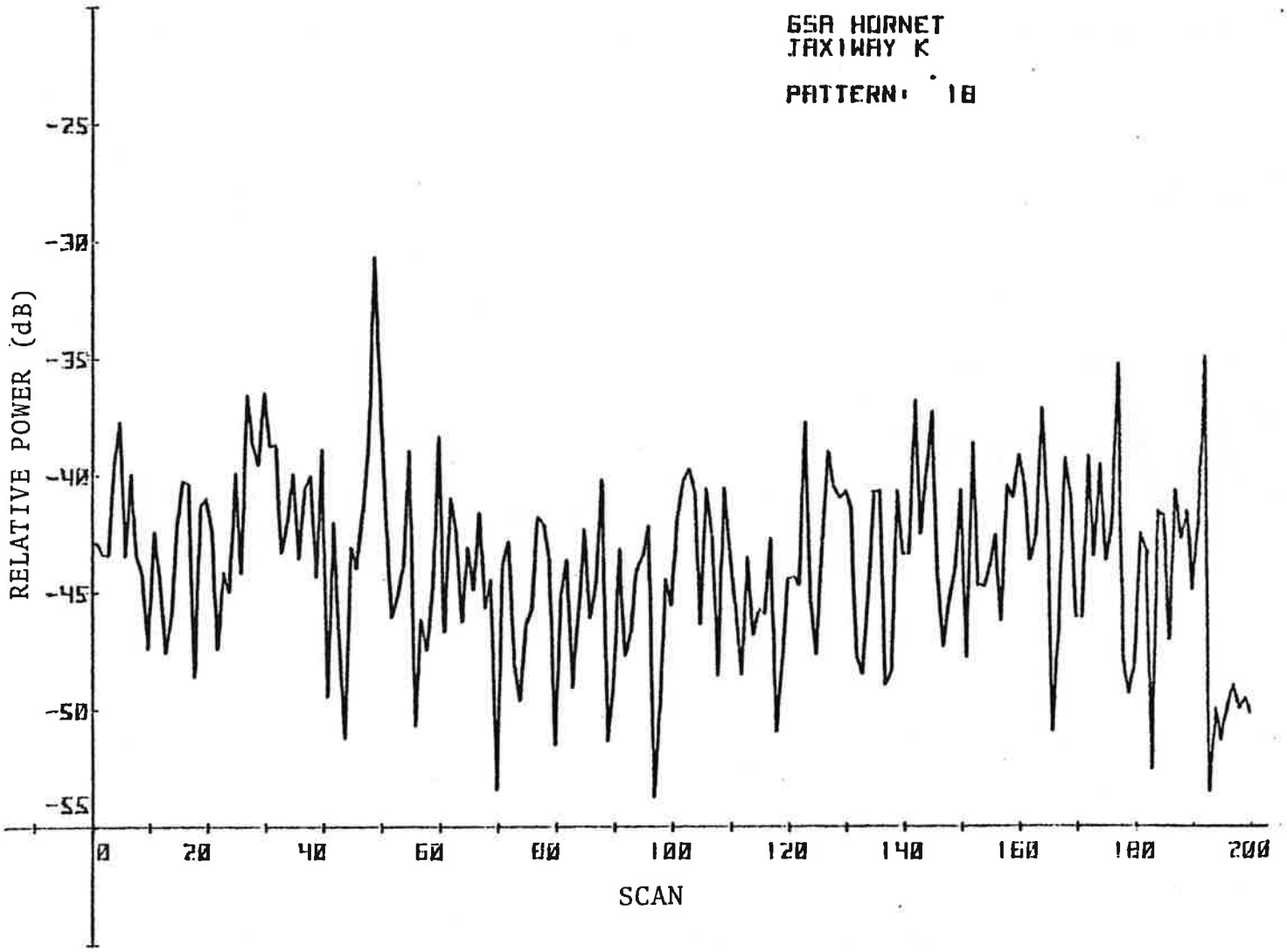

FIGURE 5.2-1. SINGLE SCAN INTEGRATED POWER RETURN FOR COMPACT CAR VS ASPECT: FIXED FREQUENCY

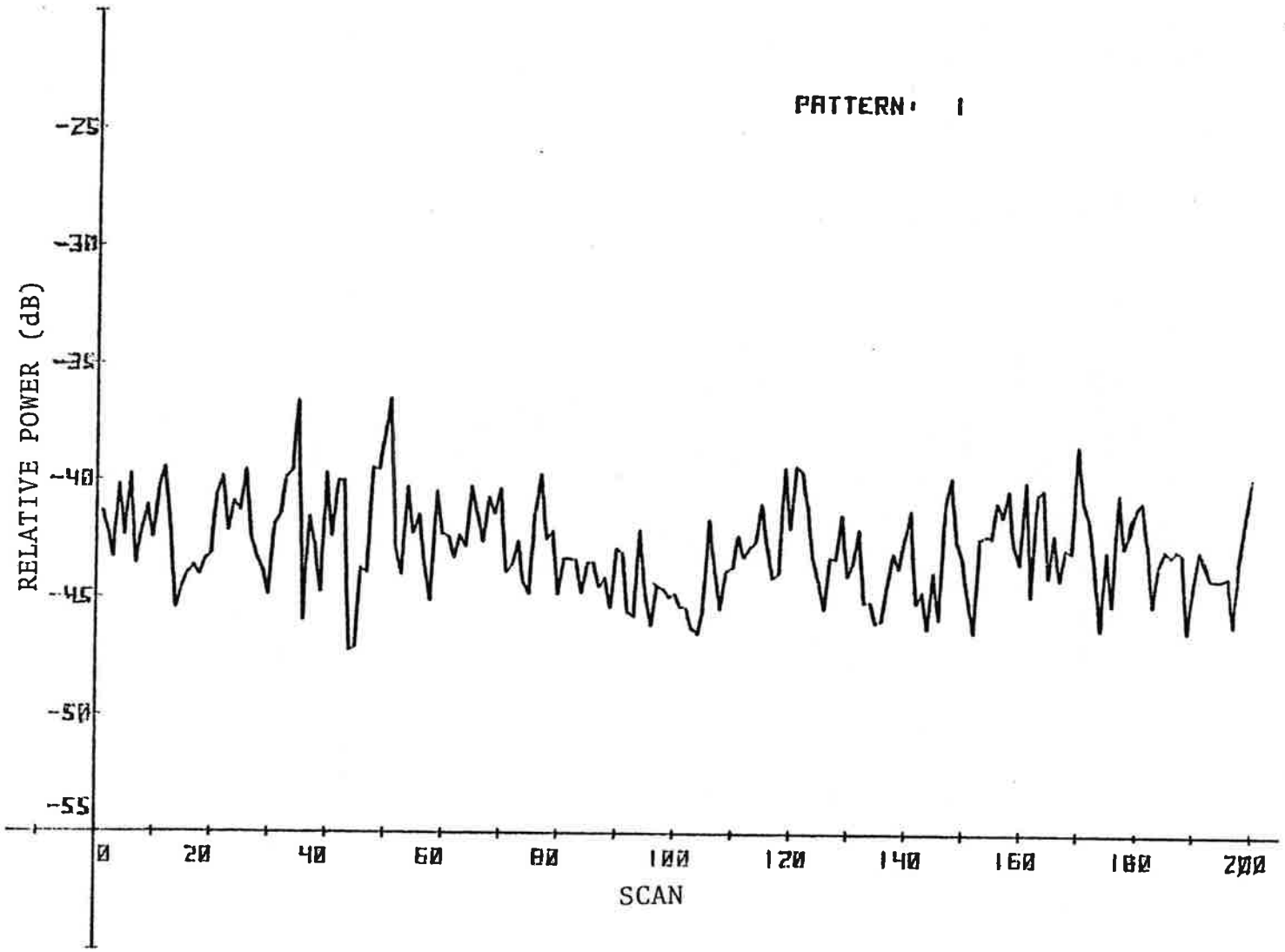

FIGURE 5.2-2. SINGLE SCAN INTEGRATED POWER RETURN FOR COMPACT CAR VS ASPECT: FREQUENCY AGILITY

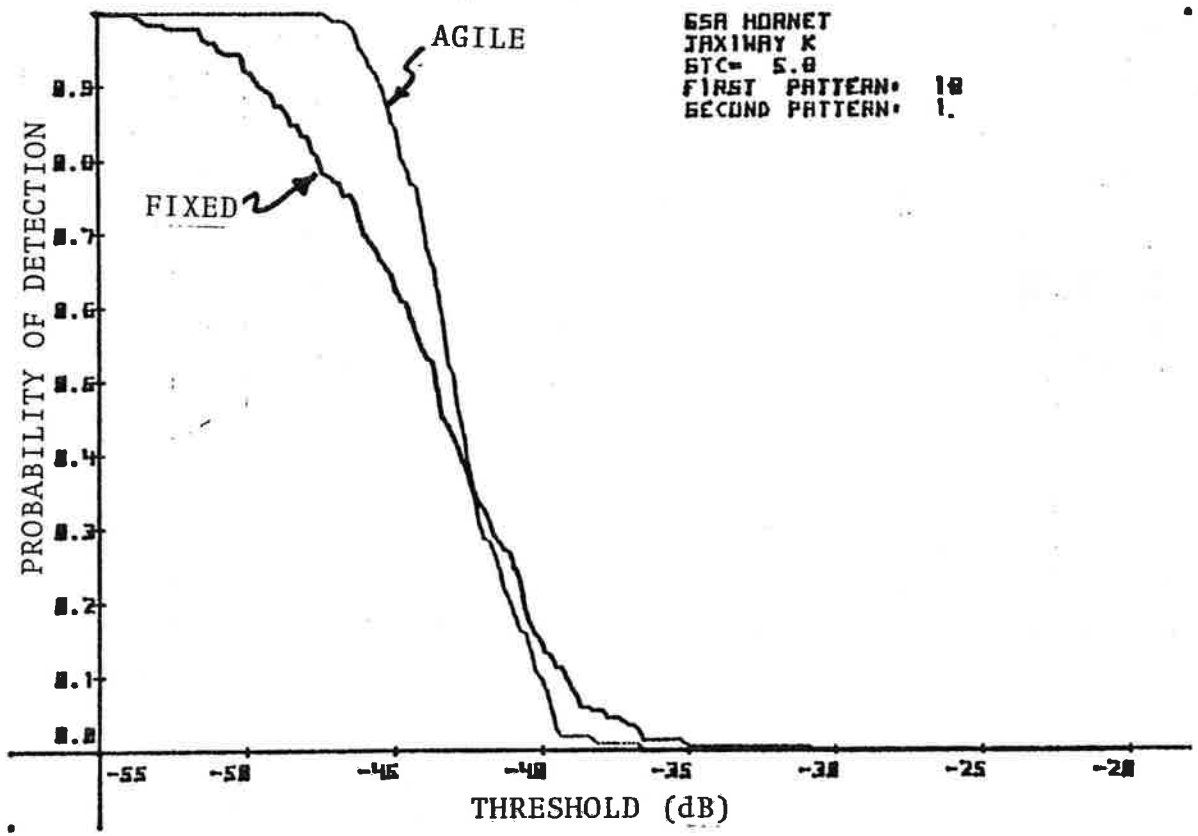

FIGURE 5.2-3. DETECTABILITY OF COMPACT CAR FOR FREQUENCY AGILITY AND FIXED FREQUENCY

TABLE 5.2-2. COMPACT CAR DETECTION PERFORMANCE IMPROVEMENT FOR FREQUENCY AGILITY

PATTERNS	BAND	P_d = 100%	P_d 90%
1	360 MHz	6.4 dB	4.1 dB
4	240 MHz	4.8 dB	3.4 dB
7	180 MHz	2.3 dB	3.8 dB
12	180 MHz	0.5 dB	3.1 dB

The 90% detectability point on the fixed frequency plot in Figure 5.2-3 corresponds to a radar cross section of $0.3m^2$, based on a comparison of signal level to the standard target RCS discussed in Section 5.1.1. This result is used in the discussion of the radar system performance model in Section 5.6.

Because the data was taken under actual operational conditions, the results are directly applicable to ASDE operational performance. The radar was scanning normally, and the vehicle was slowly changing aspect, exactly the case for a vehicle moving on a path not radial from the radar. Because a P_d of near 100% is operationally desired, the 6 dB single-scan improvement factor is a meaningful result.

Multiple-scan integration of target returns can take place if the target is moving slowly. The per-scan movement must be less than 1/2 the display resolution cell or 1/2 the vehicle length, whichever is greater. In the case of the automobile this is a speed of 10 mph or less. The effect of five scans of averaging is shown on Figure 5.2-4 for fixed frequency and on Figure 5.2-5 for frequency agility. The smoothing effect of agility is still apparent, providing a 6 dB peak-to-peak improvement and a 4 dB detectability improvement. The mean radar cross-section of the automobile begins to emerge from the fluctuation data, with a slight peak at broadside evident.

5.2.2 Small General Aviation Aircraft Detection

Data was taken with a Cherokee 180 aircraft rotated in 10° increments for a total of 180° at the far end of the FAATC ramp, about 7000 ft in range. A total of 19 frequency patterns were used to collect data for each aircraft position, representing radar spectrum occupancy from 360 MHz (maximum with additional 70 MHz guard bands) to 90 MHz. See Table 5.2-3 for the patterns used and Figure 5.2-6.

Although the data was taken in rough increments (10°), a strong indication was seen of the same fast fluctuation observed

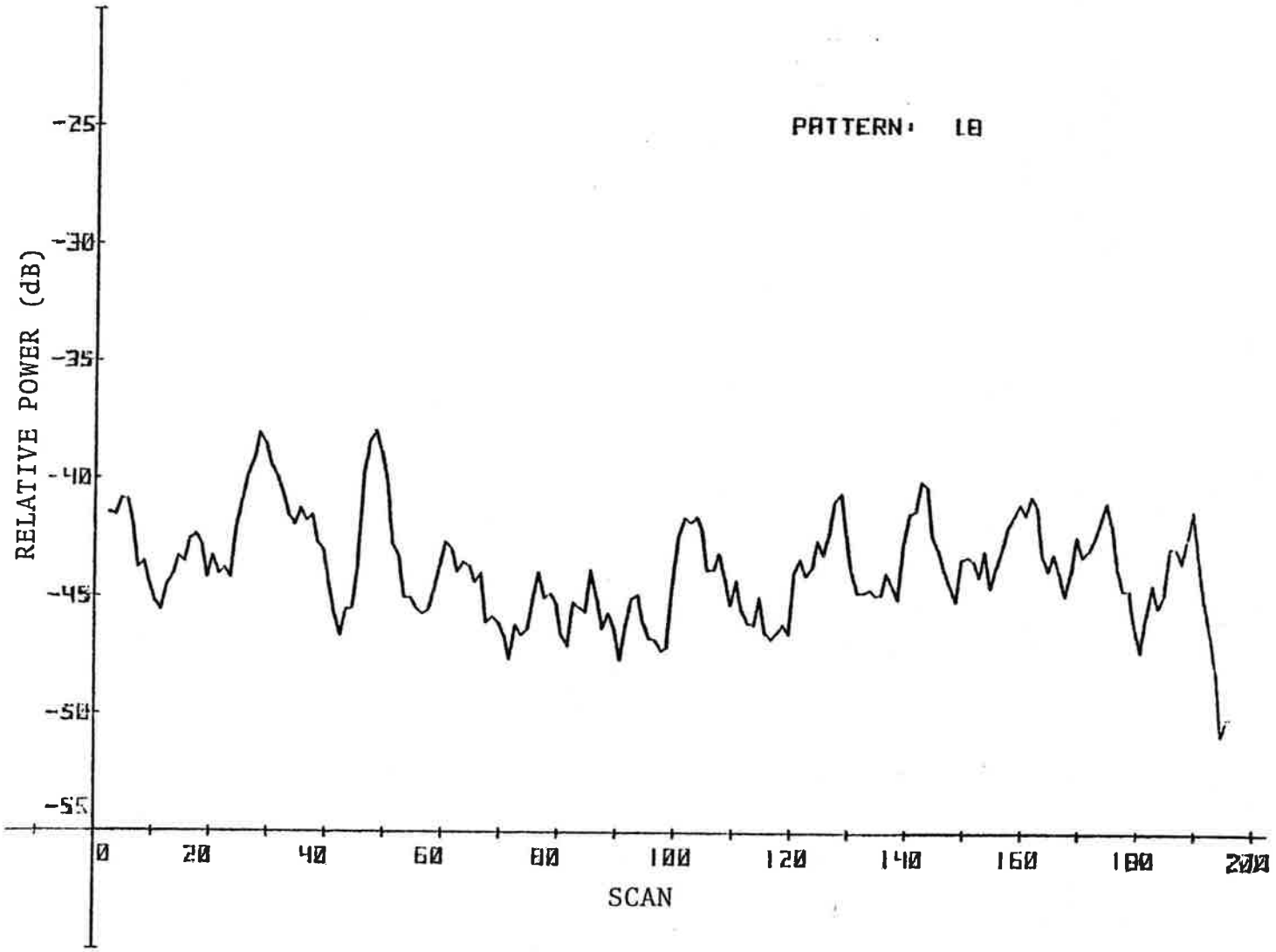

FIGURE 5.2-4. FIVE SCAN AVERAGE INTEGRATED POWER FOR COMPACT CAR - FIXED FREQUENCY

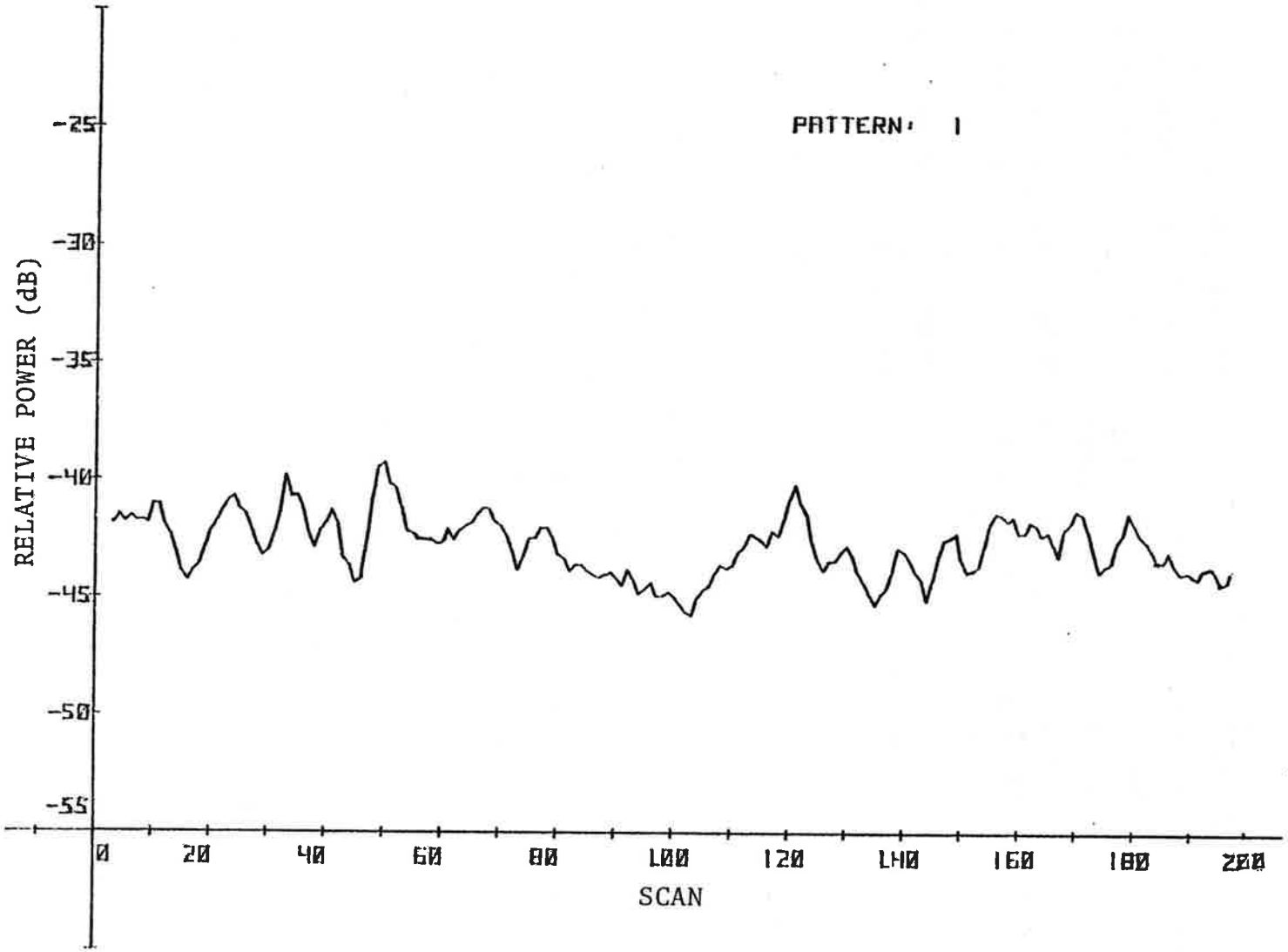

FIGURE 5.2-5. FIVE SCAN AVERAGE INTEGRATED POWER FOR COMPACT CAR - FREQUENCY AGILITY

TABLE 5.2-3. FREQUENCY PATTERNS FOR CHEROKEE 180 TEST

PATTERN	B AND OCCUPIED*	CHARACTERISTIC
1	360 MHz	13 steps, 30 MHz each, pattern A
2	360 MHz	13 steps, 30 MHz each, pattern B
3	360 MHz	2 steps
4	240 MHz	9 steps, 30 MHz each, pattern A
5	240 MHz	9 steps, 30 MHz each, pattern B
6	240 MHz	2 steps
7	180 MHz	7 steps, 30 MHz each, pattern A
8	180 MHz	7 steps, 30 MHz each, pattern B
9	180 MHz	2 steps
10	120 MHz	5 steps, 30 MHz each, pattern A
11	120 MHz	2 steps
12	180 MHz	13 steps, 15 MHz each, pattern A
13	180 MHz	13 steps, 15 MHz each, pattern B
14	90 MHz	7 steps, 15 MHz each, pattern A
15	90 MHz	7 steps, 15 MHz each, pattern B
16	90 MHz	2 steps
17	------	Fixed frequency-lower end of band
18	------	Fixed frequency-mid band
19	------	Fixed frequency-high end of band

*CENTER FREQUENCY-TO-CENTER FREQUENCY

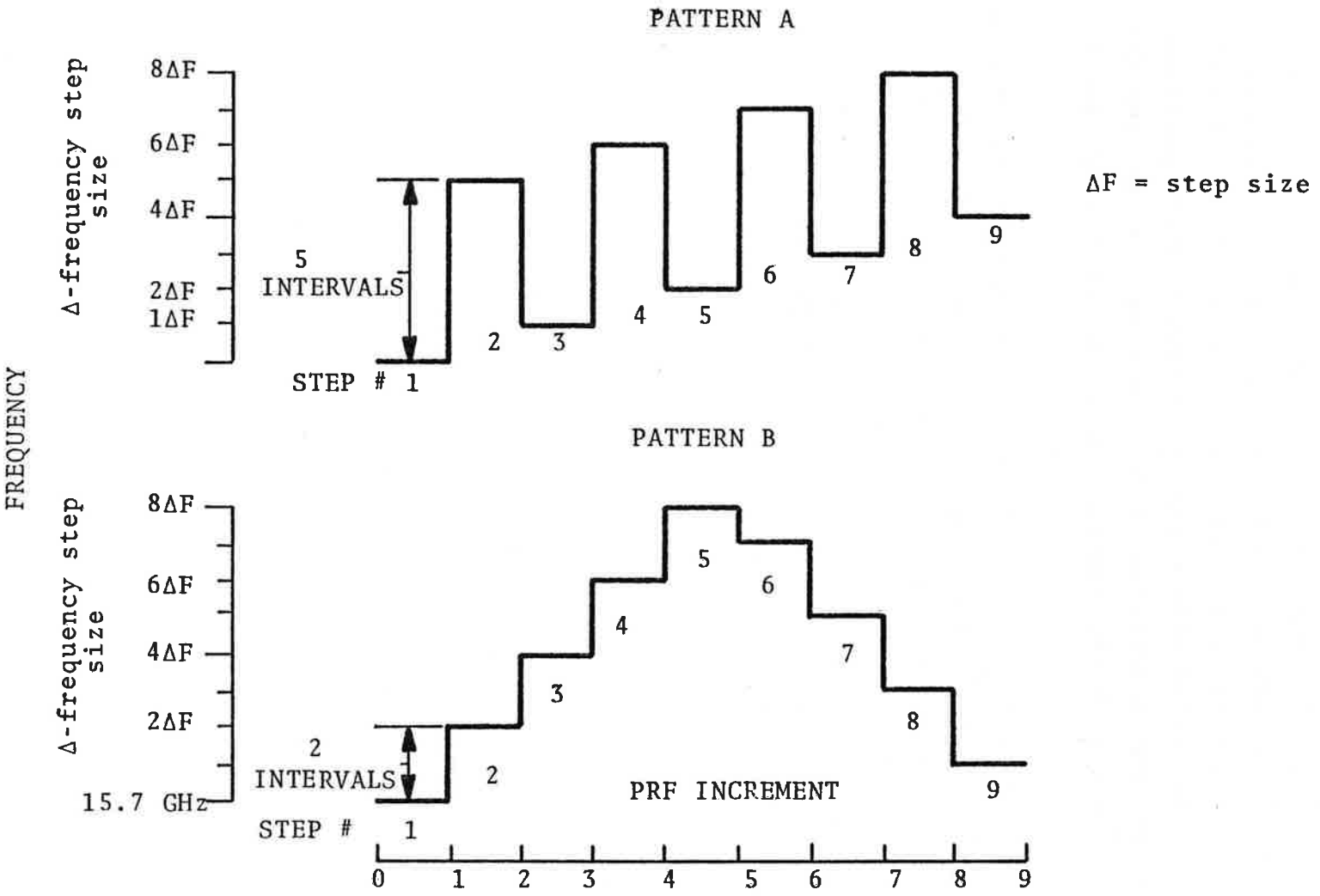

FIGURE 5.2-6. FREQUENCY AGILE PATTERN CHARACTERISTICS

for the automobile. Figure 5.2-7 plots the integrated radar return power vs. aspect for the three fixed frequency patterns. For a given aspect the radar cross section of the aircraft was seen to vary by as much as 12 dB as a function of frequency. Figure 5.2-8 is a plot of the cumulative P_d, similar to the plots described for the automobile except with much coarser quantization. The same characteristic of frequency agility is seen for the small vehicle with the improvement in detectability clearly evident.

While the data definitely shows a significant superiority of frequency agility over fixed frequency in detecting the Cherokee, the quantity of data was insufficient to conclusively establish the superiority of a particular agile pattern. The data does show, however, that there is no discernible difference between the pairs of agile patterns "A" and "B" (See Figure 5.2-6). Less than 0.2 dB difference was seen between each pair for a given agile pattern.

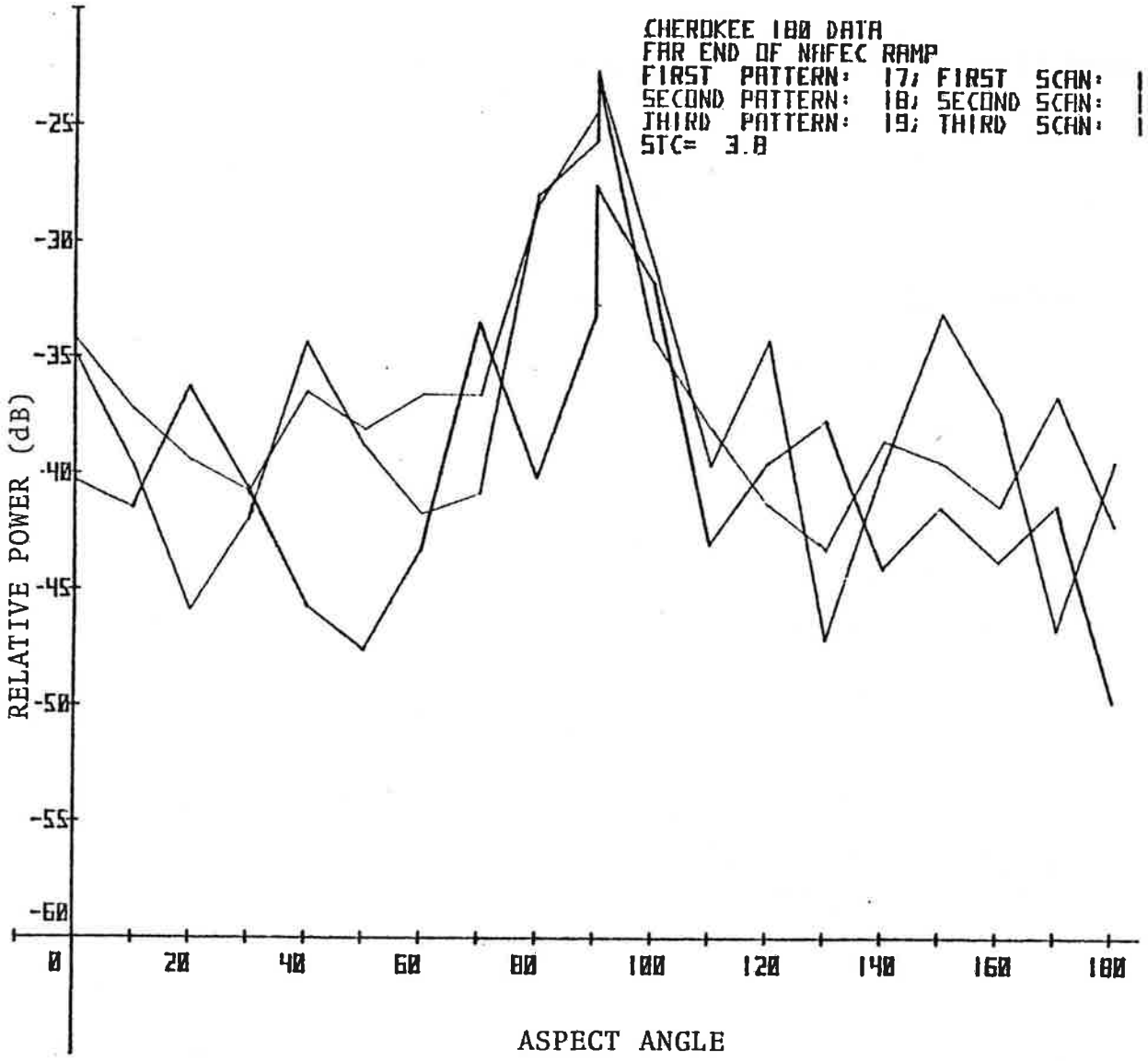

FIGURE 5.2-7. VARIATION OF TARGET RETURN POWER AS A FUNCTION OF ASPECT FOR THE CHEROKEE 180

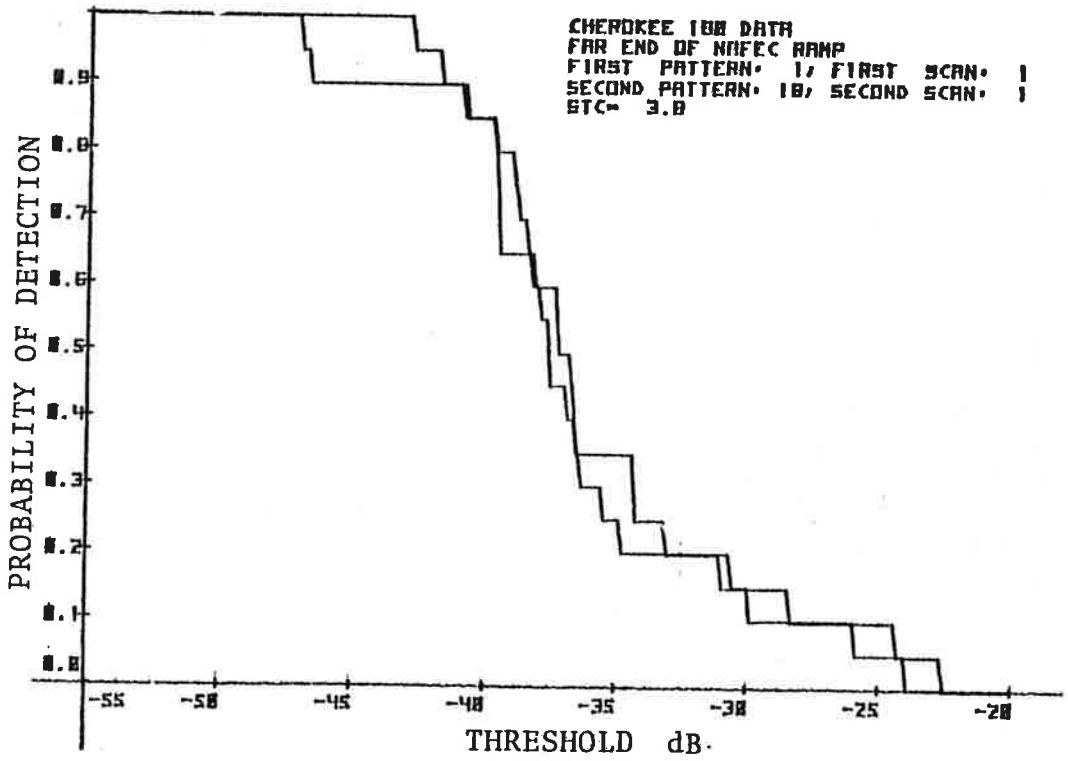

FIGURE 5.2-8. DETECTABILITY OF CHEROKEE 180 - FIXED VS AGILE OPERATION

5.3 LARGE REAL TARGET DETECTION IN CLEAR WEATHER

Test Description

To test the performance of the ASDE-3 radar in detection of large real targets, a Boeing 727 was tugged slowly through a 180° turn while the radar was continuously scanning. A full 180° turn was recorded at fixed frequency and then the turn was repeated using a 13-step frequency agile pattern. Each turn took approximately 3 minutes. This slow rate was used to observe the fluctuation in the target return for small changes in aspect angle. This test was performed at 1200' and 7000' range.

Additional tests were conducted, using a Boeing 727 and a Convair 880 to 7000', to compare the detection and imaging performance of 19 different frequency patterns. (These patterns are described in Section 5.2.2). The aircraft were positioned at 10° intervals in aspect angle and data was collected for each of the 19 frequency patterns at each aspect angle.

Test Results - Detection

At 7000', over continuous 180° turns, the total power returned from the 727 varied 9.75 dB for fixed frequency and 7.5 dB for frequency agile. This data is plotted in Figures 5.3-1 and 5.3-2, respectively. The target fluctuation vs aspect angle was slower and of smaller extent for frequency agility. This appears in the smoother nature of the plot in Figure 5.3-2.

Although there is an improvement in peak-to-peak fluctuation for this large target, this improvement does not benefit the level at which a detection threshold could be set, (as was the case for the small real targets) since that threshold would be set on the returns expected from the weakest targets that are to be detected.

The reduction in fine grain fluctuation (smoother curve) and peak-to-peak fluctuation due to frequency agility demonstrates that use of frequency agility gives a more stable target image brightness on a scan-to-scan basis as large targets are rotated.

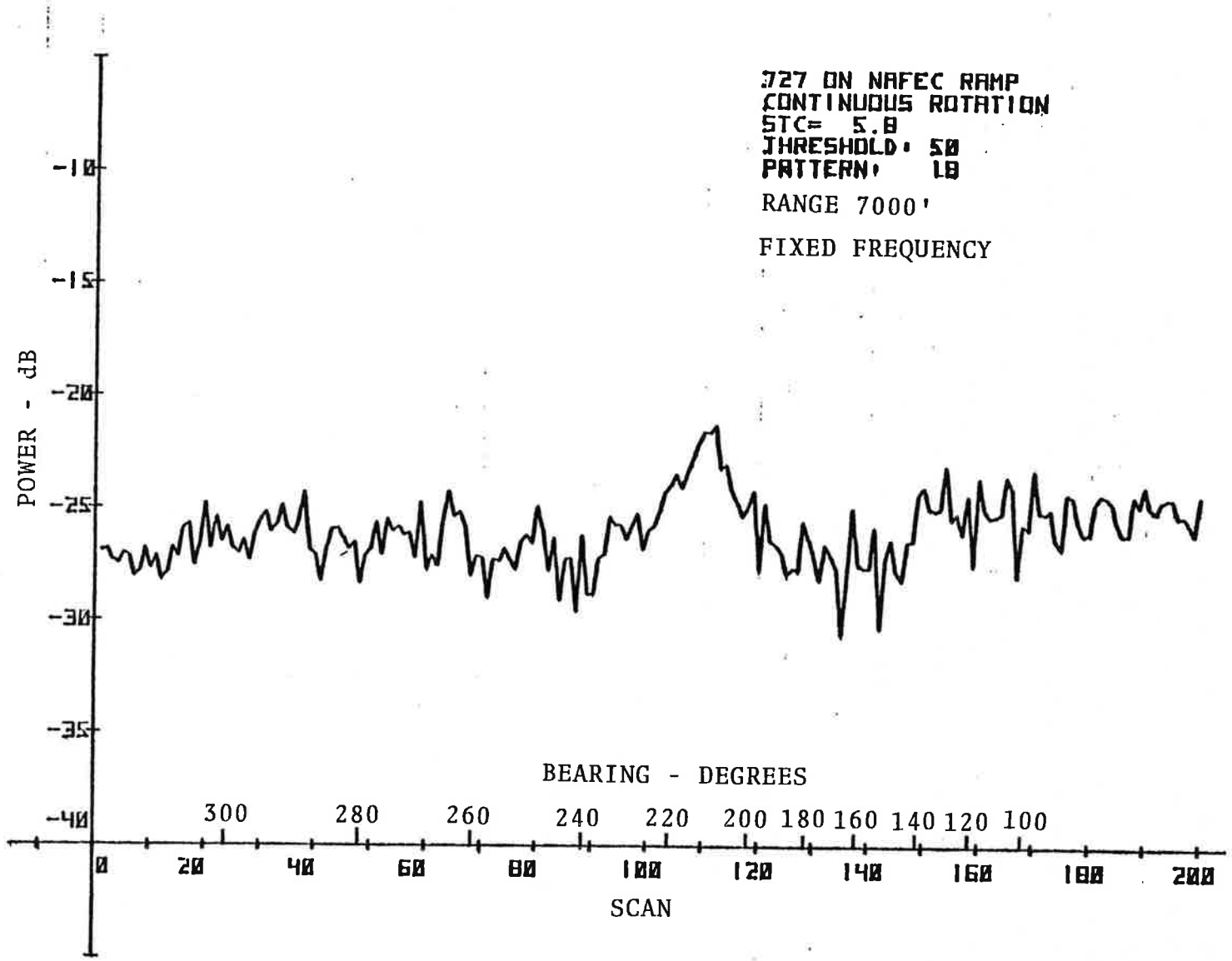

FIGURE 5.3-1. TOTAL POWER RETURNED FROM 727 DURING SLOW 180° TURN - FIXED FREQUENCY

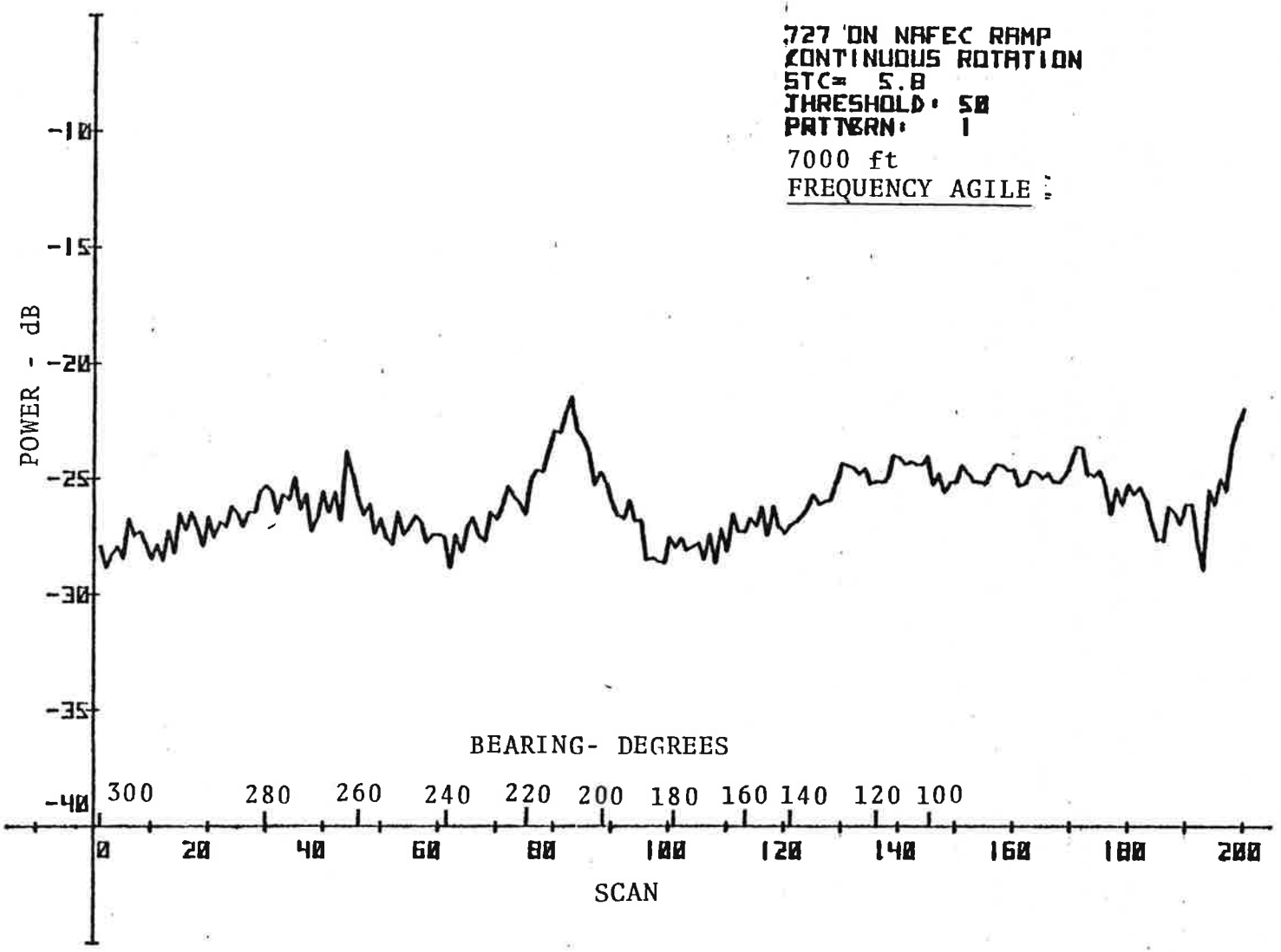

FIGURE 5.3-2. TOTAL POWER RETURNED FROM 727 DURING SLOW 180° TURN – FREQUENCY AGILE

Test Results - Imaging

The data from the 727 continuous rotation at 7000' were processed and printed as target images, as they would appear on the display. Because of the fact that the spacing between radar pulses is much smaller than the display spot size at these ranges, this reduction process includes integration over several pulses. This integration which occurs in the display system during live operation, in combination with the use of frequency agility, was theoretically expected to result in a "filling in" of nulls in the distributed target image.

A manual analysis of the printed data showed that the body of the target "broke" or separated 43% of the time with fixed frequency and 29% of the time with frequency agility. This is 33% reduction in "target breakup" occurrence with frequency agility. Figure 5.3-3 shows a sample of the image printouts.

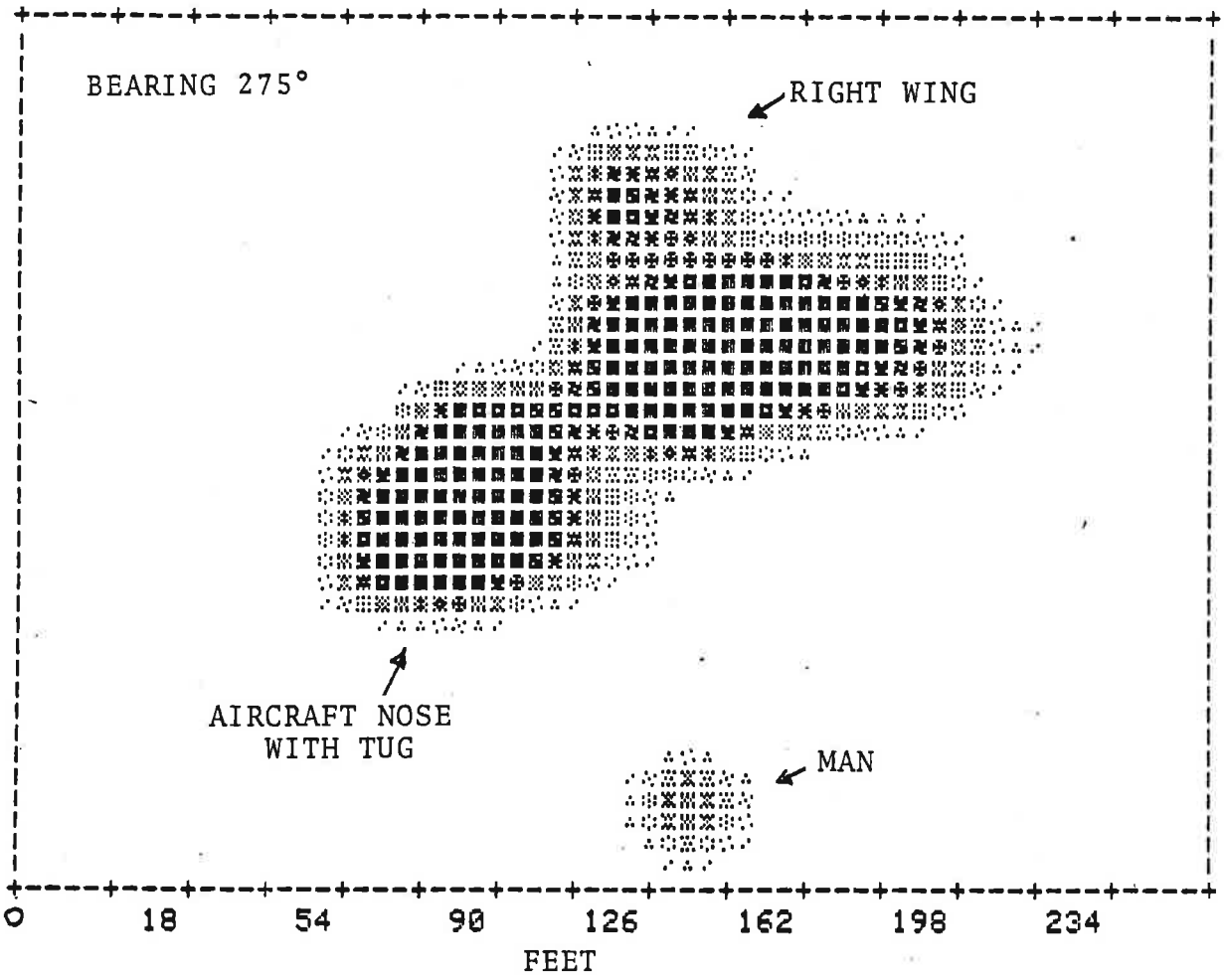

FIGURE 5.3-3. SAMPLE IMAGE OF BOEING 727 AT 7000 FEET

5.4 DETECTION PERFORMANCE IN RAIN

The rain performance tests conducted had the following objectives:

1. Verify the analytical detection performance model using field data.
2. Determine the benefits of frequency agility over fixed frequency operation in detecting targets in rain clutter.

The test set-up for the rain performance tests included the following:

- Paved pads were installed at 476, 4846 and 8504 feet. Each paved pad was large enough in range-azimuth extent to allow the placement of reflectors on each pad, and still have sufficent area for measuring returns from the paved area only, (considering the radar's antenna pattern, the transmitted pulse width and range to the pad).
- Reflectors, as discussed in the radar cross-section measurement section of this document, were installed on each pad; one reflector on pads 1 and 3, and 2 reflectors on pad 2.
- A rain gauge, capable of sensing instantaneous rain rate, was installed at the rear of each pad, with communication lines to the radar site.

The characteristics of the radar were measured. These characteristics included system losses, antenna patterns, transmitter power, noise figure, and receiver parameters. The Data Acquisition Subsystem, (DAS), was calibrated for the receiver's voltage-to-power received transfer function.

Data was recorded every 2 seconds (every other radar scan) with the radar alternated between fixed frequency and frequency agile operation. This procedure was designed to come as close as possible to obtaining data that compares fixed frequency performance with frequency agile performance for identical rainfall conditions.

A limited amount of rainfall data was obtained due to time constraints, the majority of the data was obtained at pad 2.

5.4.1 Analytical Model Verification

Target and paved area radar return data were recorded during a rainstorm. The target used represents a non-fluctuating target. The return from this type of target should basically be of a singular value, varying only in amplitude due to attenuation and any changes in the multipath environment induced by the rainfall. The return from the paved area represents the rain clutter echo power since the paved area's clear weather return was close to system noise level.

The integrated clutter return mean (average) power value, at the same rainfall rate, is the same for frequency agile and fixed frequency operation, when calculated over a region large enough to average spatially decorrelated samples. But the standard deviation of the distribution of the clutter return is reduced by frequency agile operation. Consequently, although the average target-to-rain clutter ratio is the same for both fixed and frequency agile, frequency agility does improve the single scan false alarm rate and probability of target detection for a particular detection threshold level. This improvement will be discussed in the following section. This section addresses the average target-to-rain clutter ratio and the improvement in target detection capability measured in the field, and compares this data with the analytical model predictions.

Data Processing

The rain clutter data from the paved area was calibrated to give corresponding power at receiver input, integrated over several pulses (as the display does) and a mean and standard deviation value in dBm was obtained for each radar scan that was recorded. The target return on that scan was likewise integrated over several pulses. Attenuation was calculated as the ratio of the current target return to the target return when the rainfall rate was

approximately zero. Signal to noise-plus-clutter (S/(N+C)) was calculated as the ratio of the mean target return to mean noise-plus-clutter return.

Test Results - Attenuation

A plot of mean attenuation vs rainfall rate for pad 2 is presented in Figure 5.4-1. Each point represents an average of several radar scans (from 4 to 40 seconds) of data, when the rainfall rate and attenuation were approximately steady. The bar at each point represents the one sigma spread of the data.

An attenuation curve for pad 2, analytically derived from the radar system parameters is plotted with the empirical mean attenuation data in Figure 5.4-1. It is apparent that the observed attenuation exceeds the theoretical prediction by about 5 dB. Several factors can account for this discrepancy. First, the data was taken during a thunderstorm where, the common expression for reflectivity of rain becomes inaccurate.* Second, the Rayleigh scattering model applies only to a portion of the raindrops (those <1.3mm) at these frequencies, 'Mie' scattering applies to the rest, and Mie scattering can result in up to twice the scattering as Rayleigh.** (The model used for our attenuation curve assumes Rayleigh scattering, and no thunderstorm). Third, other attenuation measurements at 1.25 cm (ASDE is 1.8 cm) generally showed greater attenuation than the model predicted.† The discrepancy for the first factor is up to 1.5 dB and for the second is up to 3 dB. So the measured data is not unreasonable.

The scatter in the data is probably due primarily to spatial variation in rainfall rate and drop size.†

*AFCRL Handbook of Geophysics, 1969, p 9-20.

**Battan, Radar Observations of the Atmosphere, p 40, 41.

†Battan, op. cit., p 73.

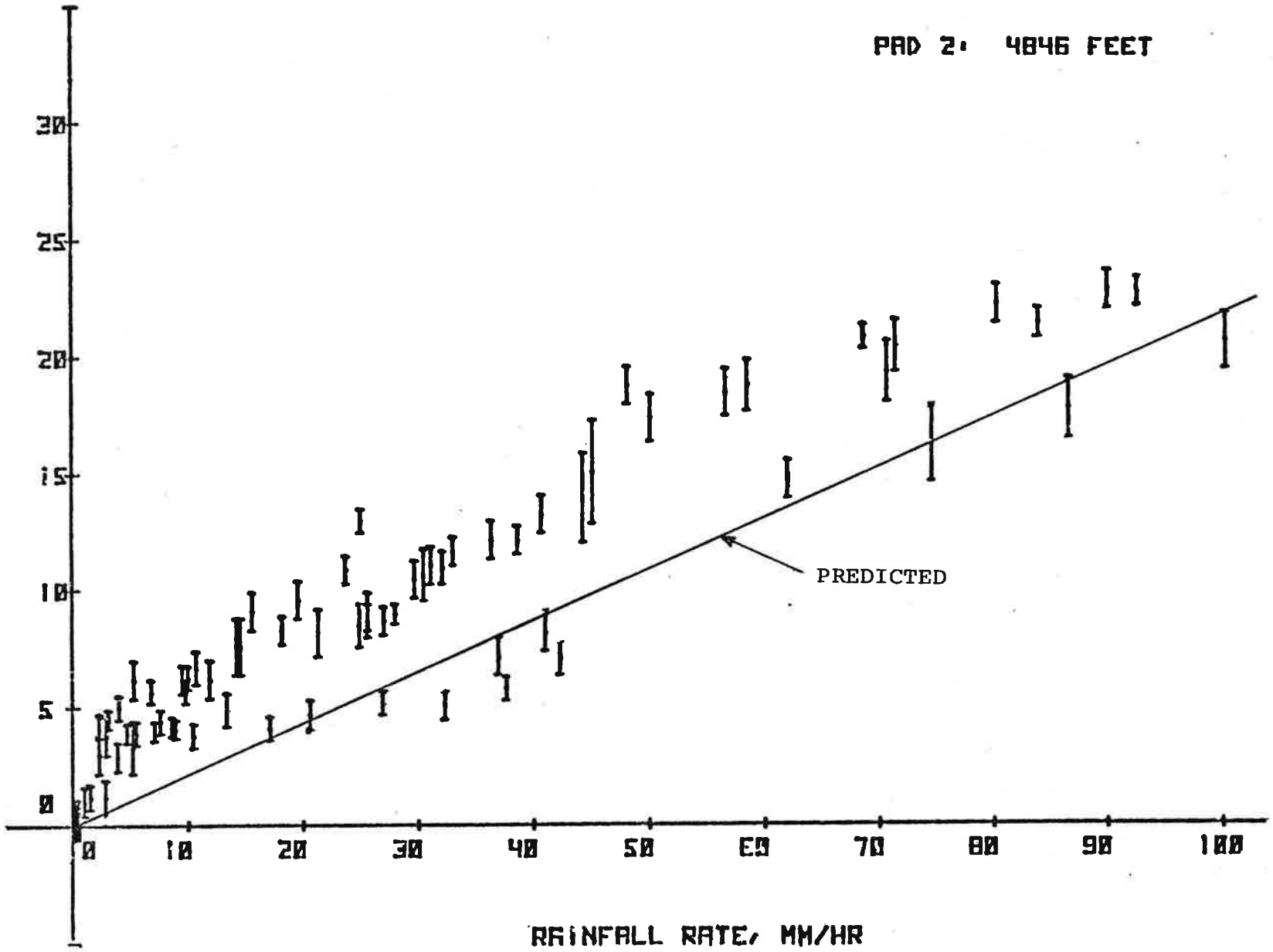

FIGURE 5.4-1. ASDE-3 ATTENUATION VS RAINFALL RATE

Test Results - Signal To Noise-Plus-Clutter (Average)

Plots of the mean signal to noise-plus-clutter for pads 2 and 3 are presented in Figures 5.4-2 and 5.4-3, respectively. Each point in these plots represents an average of several radar scans (from 4 to 40 seconds) of data, when the rainfall rate and attenuation were approximately steady. The bar at each point represents the one sigma spread in the mean clutter return for fixed frequency at that point.

S/(N+C) curves, analytically derived from the radar system parameters, are plotted with the empirical mean S/(N+C) data. The slope and shape of the analytical curves appear to fit the empirical data fairly well. The scatter in the empirical data is probably due to the spatial variation in rainfall and the fact that variation in drop size affects attenuation but is not necessarily correlated with rainfall rate. Significant spatial variation in rainfall was observed. Seldom was the rainfall rate the same at any two of the test pads (separated by 4000') and even within the area of a pad itself, the rain sometimes is highly variable.

5.4.2 Detection in Rain Clutter

Measurements on fluctuating targets were taken in clear weather, (see the sections on small and large real target detection), showing the improvement in target detection resulting from frequency agility operation. In rain, a fluctuating target will benefit from the same improvements seen in clear weather plus the improvement derived from frequency agility in reducing the dispersion of the integrated rain clutter. Since it is difficult to characterize and construct a standard fluctuating target, a simple non-fluctuating target was used in the rain experiments. Non-fluctuating targets, because they appear as a singular scatter, do not benefit from frequency agility.

Improvements in target detection in rain due to frequency agility operation occur because on each pulse a statistically

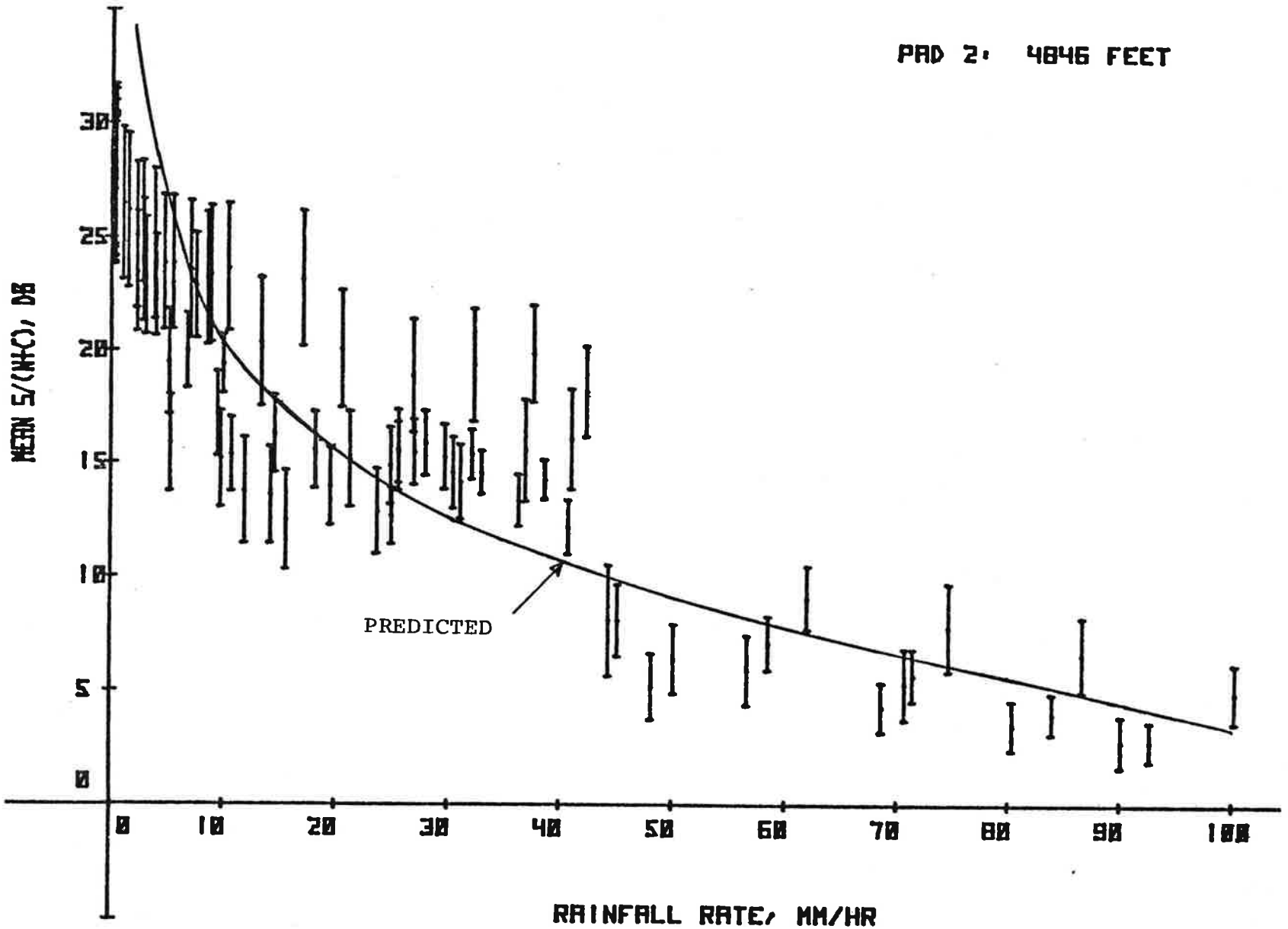

FIGURE 5.4-2. ASDE-3 S/(N+C) PERFORMANCE VS RAINFALL RATE, AT 4846 FEET

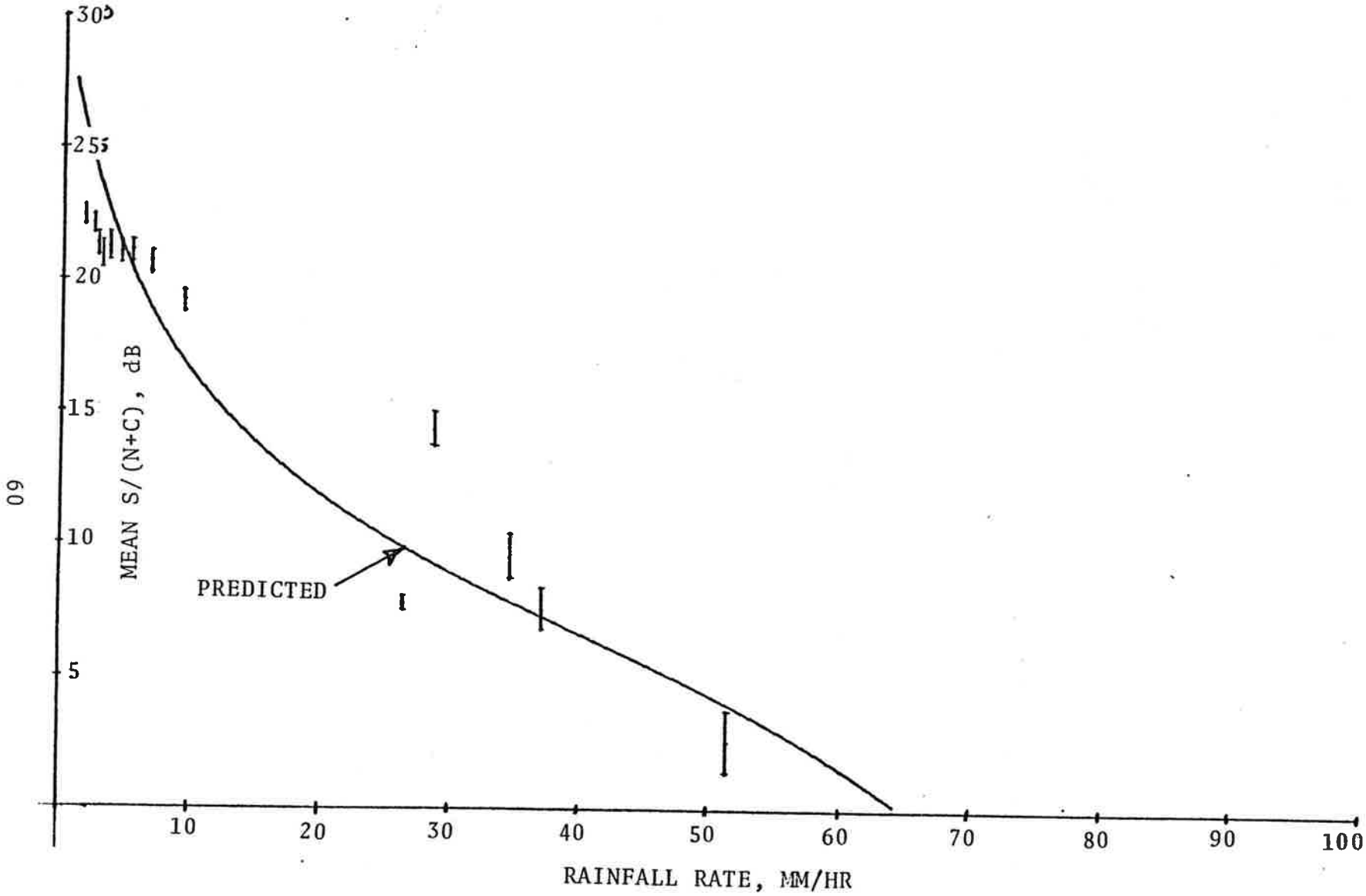

FIGURE 5.4-3. ASDE-3 S/(N+C) PERFORMANCE VS RAIN RATE, AT 8504 FEET

independent sample of the rain clutter is obtained and when several adjacent samples are integrated, the resultant value has a much lower variance than it would if the samples were statistically dependent. This reduced variance allows a lower received signal threshold to be maintained for a given probability of false alarm, thereby improving the probability of target detection. Figure 5.4-4 gives one example of the rain clutter distributions for frequency agile and fixed frequency operation. The data for this figure was taken at a time when the rain rate was 73 mm/hr.

Note on Figure 5.4-4 that if a threshold is set at the point where the integrated clutter returns are zero (probability of false alarm of 'zero' for the data population) then there is a difference of approximately 2.7 dB between fixed frequency and agile thresholds. This represents the improvement in detection for frequency agility for the particular set of data used.

Figure 5.4-5 shows for the same data the probability of false alarm due to rain clutter versus target detection threshold location for fixed and frequency agile operation. This figure also shows the 2.7 dB improvement at the 'zero' false alarm level. This 'zero' false alarm level is used later in processing and analyzing the data. It should be noted here that the number of samples taken, approximately 1000, does not allow a probability of false alarm of 10^{-6} to be evaluated (the value used for theoretical prediction). The point chosen for the processing and analysis is convenient, but indicates that only one sample in a thousand was at the threshold, (a probability of false alarm of 10^{-3}).

The benefits of frequency agility at a given rainfall rate can be expressed as a reduction in the threshold level required to obtain the same false alarm probability as that obtained using fixed frequency. As described above, the threshold was placed just above the maximum integrated clutter return which represents 'zero' probability of false alarm for the approxima-

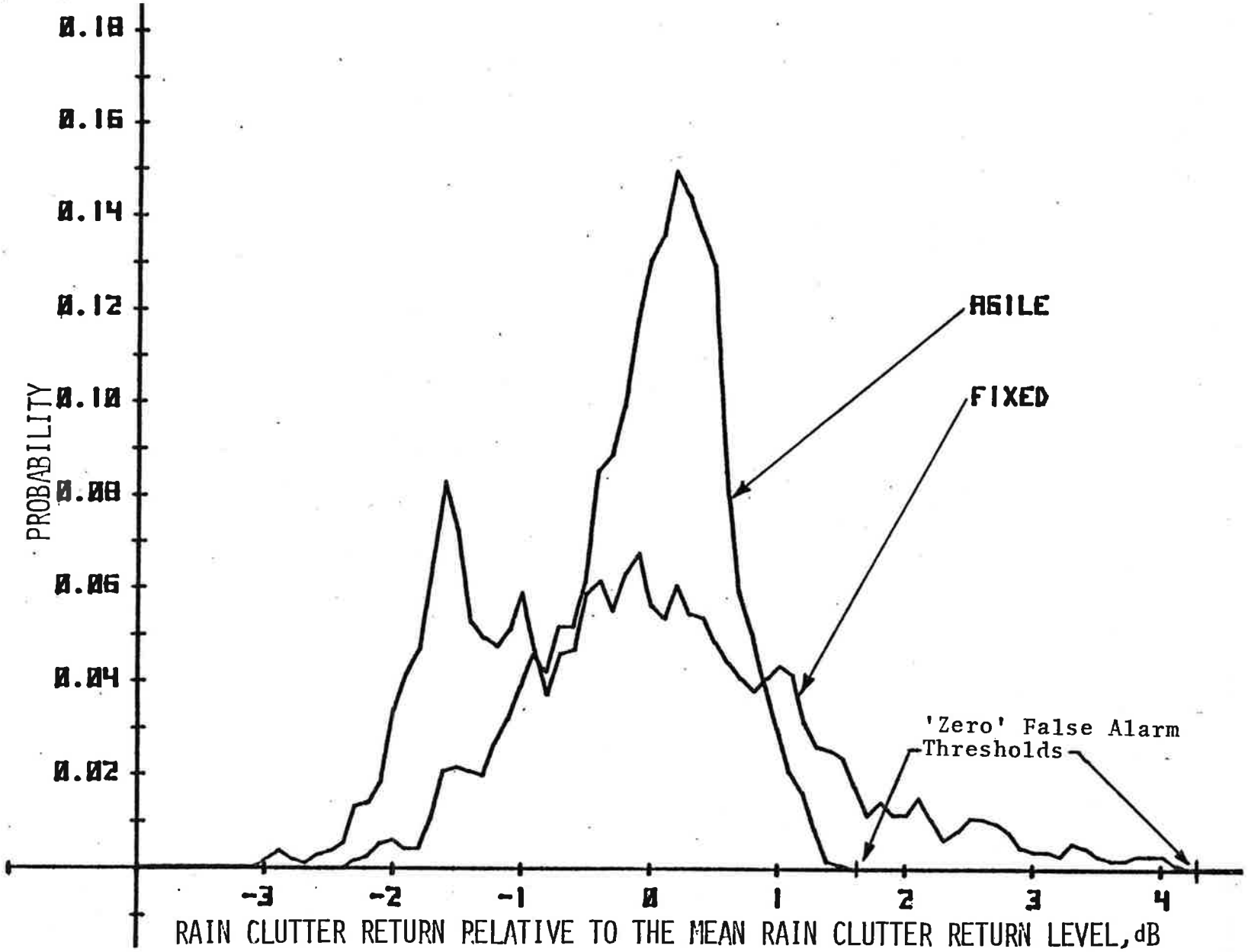

FIGURE 5.4-4. FIXED FREQUENCY & FREQUENCY AGILE RAIN CLUTTER DISTRIBUTIONS AT 73 MM/HR

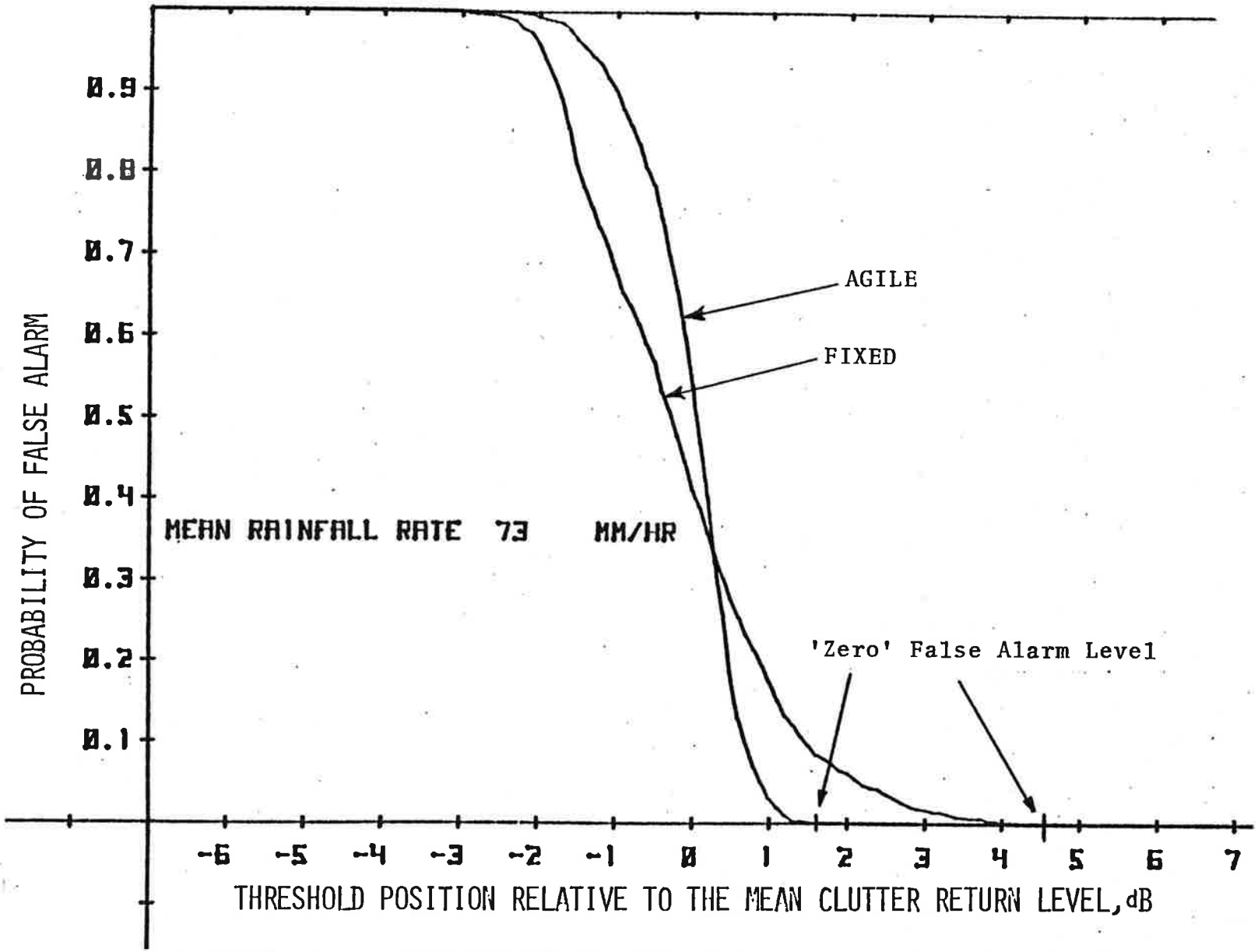

FIGURE 5.4-5. PROBABILITY OF FALSE ALARM DUE TO RAIN CLUTTER VS TARGET DETECTION THRESHOLD LOCATION, FIXED FREQUENCY AND FREQUENCY AGILE

tely 1000 samples taken on each scan.

The data was collected on a scan-to-scan basis, one scan of fixed frequency data followed by one scan of frequency agile data two seconds later. The rainfall rate during this time interval (approximately 2 seconds) changed very little. The outputs from the receiver for the range-azimuth resolution cell were integrated by taking the arithmetic sum of the measured voltages.*

The equation for the improvement in detection performance due to frequency agility, P_a expressed in dB, is given by the following equation.

$$P_a = 20 \log \frac{T_{CF}}{T_{CA}}$$

where

T_{CF} - is the threshold required for fixed operation,

T_{CA} - is the threshold required for agile operation, and the thresholds in both cases, fixed and agile, are set just above the maximum integrated clutter level, (a probability of false alarm of 'zero' for the data evaluated.)

The improvement in target detection for the radar system evaluated due to frequency agility (as determined by the above process) is shown in Figure 5.4-6. The typical benefit for the radar system evaluated is two to three dB. The improvement presented is limited by the radar system's noise floor. The rain clutter signal returns from the test pads were highly attenuated by the rain-induced path loss, and were received at a level where system noise competed with the rain clutter

*Marcum and Swerling, Studies of Target Detection by Pulsed Radar, 1960, pp 73-74.

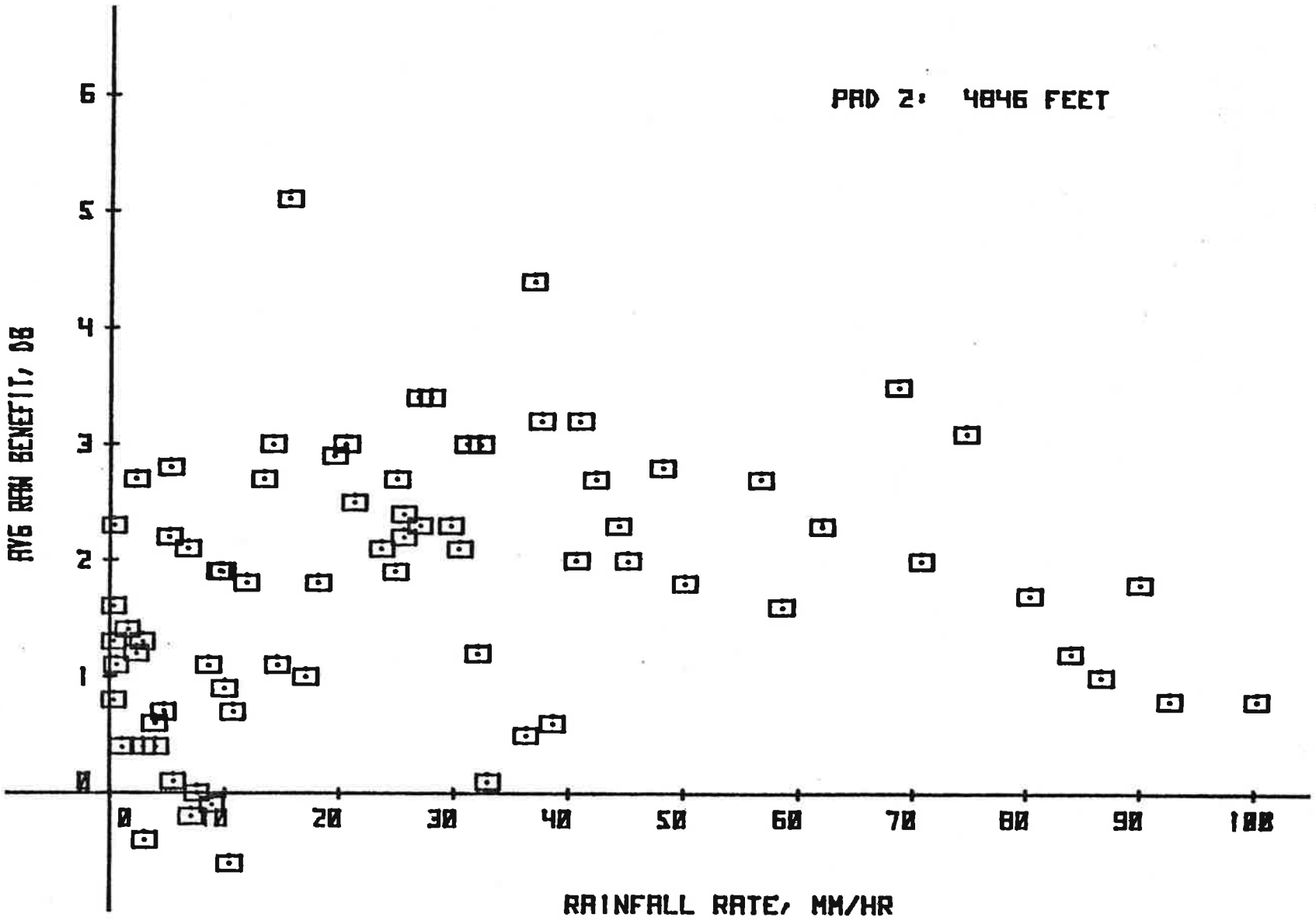

FIGURE 5.4-6. IMPROVEMENT IN TARGET DETECTION DUE TO FREQUENCY AGILITY-UNADJUSTED

returns. Consequently, the benefits shown in Figure 5.4-6 fall short of the predicted theoretical benefits because of limitations in the evaluated radar system.

The improvement in target detection without system noise limitations was evaluated by further data processing to allow a better comparison against the predicted theoretical benefits. The mean system noise level was subtracted from the data. Since the noise term in noise-plus-clutter not only affects the location of the mean noise-plus-clutter, but also contributes to its standard deviation, the threshold point for a probability of false alarm equal to 'zero' was moved lower in value. The assumption was made that the noise increased the threshold in proportion to its effect on the standard deviation.

This proportion is developed below:

σ_{C+N} = standard deviation of noise-plus-clutter

$$= \sqrt{\sigma_C^2 + \sigma_N^2} \quad ;$$

where

σ_C is the standard deviation of clutter and

σ_N is the standard deviation of noise

$$\sigma_C = \sqrt{\sigma_{C+N}^2 - \sigma_N^2}$$

$$\frac{\sigma_C}{\sigma_{C+N}} = \sqrt{\frac{(\sigma_{C+N})^2 - (\sigma_N)^2}{(\sigma_{C+N})^2}}$$

The threshold relative to the mean is assumed to change by the preceding proportionality factor. Additionally, the effect of small rain rate variations between adjacent samples is compensated for by subtracting out the difference between the mean values of the two samples. It is assumed that there are only minor changes in threshold relative to the mean for small changes in rainfall rate.

The equations used to compensate threshold for radar system noise are given below. The values determined by these equations are used in the P_a equation previously defined to calculate improvement.

$$T_{CA} = \left(M_{C+N_A} - M_N\right) + \left(T_{C+N_A} - M_{C+N_A}\right) \sqrt{\frac{\sigma^2_{C+N_A} - \sigma_N^2}{\sigma^2_{C+N_A}}}$$

$$T_{CF} = \left(M_{C+N_A} - M_N\right) + \left(T_{C+N_F} - M_{C+N_F}\right) \sqrt{\frac{\sigma^2_{C+N_F} - \sigma_N^2}{\sigma^2_{C+N_F}}}$$

where:

T_{C+N} = target detection threshold set just above maximum noise-plus-clutter level

M_{C+N} = mean integrated noise-plus-clutter

σ_{C+N} = standard deviation of integrated noise-plus-clutter

M_N = mean integrated noise (no clutter)

σ_N = standard deviation of integrated noise (no clutter)

M_C = mean integrated clutter (no noise)

σ_C = standard deviation of integrated clutter (no noise)

Figure 5.4-7 shows the improvement in target detection adjusted for noise and change in mean clutter. The benefits shown are typically 4 to 5 dB. This result is based on a probability of false alarm of 10^{-3} as described above, in the discussion of Figure 5.4-5. Adjusting for a probability of false alarm of 10^{-6} by using a Rayleigh distribution improves the benefit by approximately 1 dB to a range of 5 to 6 dB, which is below the theoretical prediction of 8.8 dB for Rayleigh scattering. However, the scattering observed probably consisted only

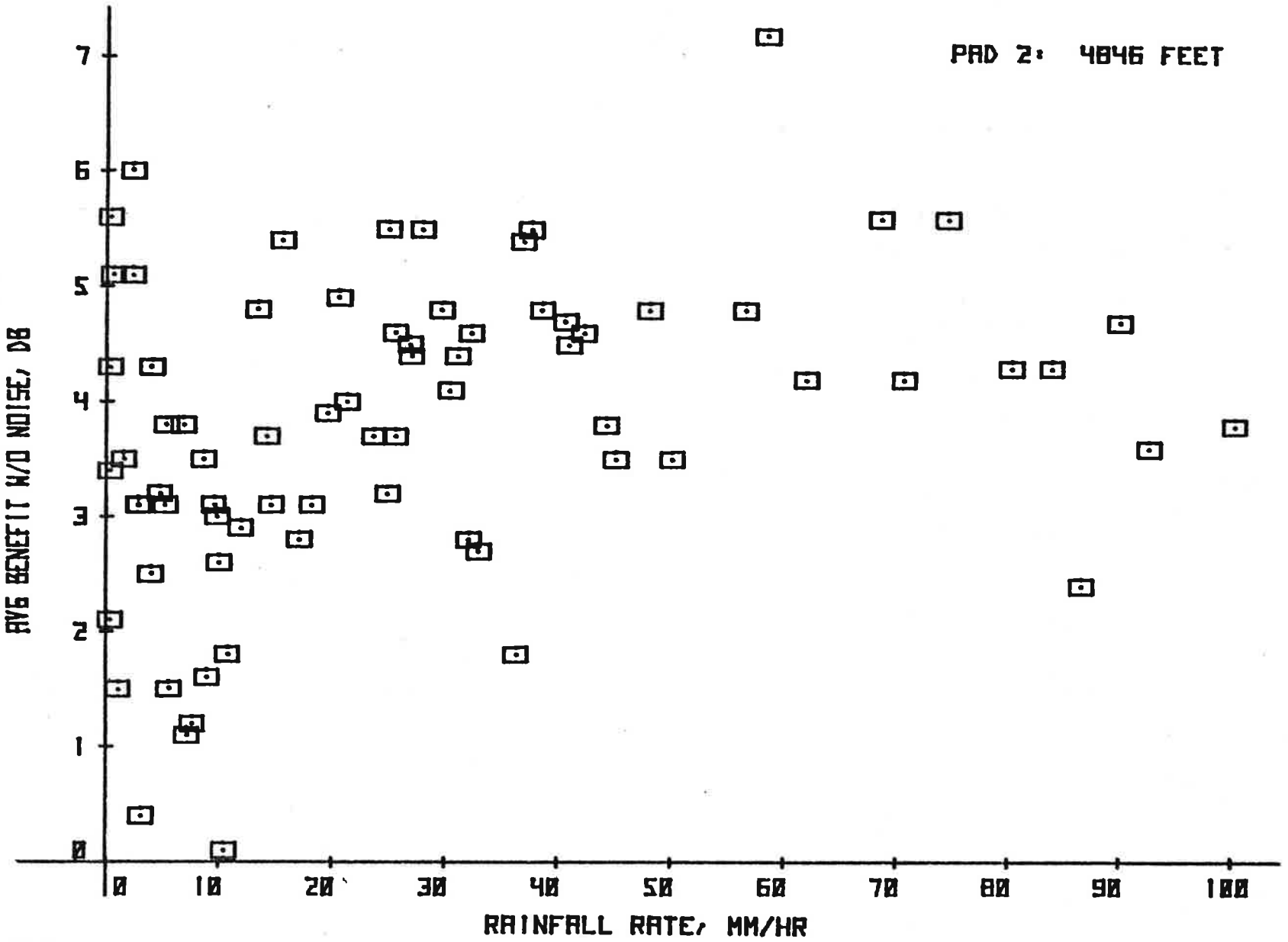

FIGURE 5.4-7. IMPROVEMENT IN TARGET DETECTION DUE TO FREQUENCY AGILITY ADJUSTED FOR NOISE AND CHANGE IN MEAN CLUTTER

partially of Rayleigh scattering, as is described in Section 5.4.1, under 'Test Results - Attenuation'.

5.4.3 Qualitative Detection Improvement Due to Frequency Agility

During the time that the ASDE-3 radar beam is dwelling on a target, any rain that is in the beam is essentially 'frozen'. The dwell time is approximately 0.7 milliseconds, whereas several milliseconds would be required for the rain to have moved far enough to appear different to the radar.

For a particular frequency there will be spatial regions where the arrangement of drops is such that the reflected power from the drops adds and the clutter return will be enhanced. If the drops were re-arranged (by waiting long enough, for example) the reflected signals would no longer add but might cancel. The same effect could be achieved by using a different frequency which has a sufficiently different wavelength to cause the drop arrangement to 'look' different to the radar as far as addition or cancellation is concerned.

For fixed frequency operation, as the radar beam scans by a region where the returns add, the returns will be enhanced for each pulse that hits that region. This is so because the dwell time is short enough that the drops have effectively not moved and because the frequency has not changed. The return would actually look like a bright 'spot', like a small target.

For frequency agility operation, each radar pulse uses a new frequency, (for as many pulses as there are steps in the pattern), and the rain looks to this new frequency as if it had been completely rearranged. Thus any strong returns from rain should persist in azimuth for only one radar pulse, not several like a small target would. This is exactly the observed effect!

Figure 5.4-8, in the top pair of illustrations, shows a raw data comparison of fixed and agile operation. Each horizontal line of the graphical printout represents a single radar pulse. For fixed frequency, clumps of returns appear like small

RAINFALL RATE: 6 mm/hr (ALL DATA SPECIALLY PROCESSED TO ENHANCE RAIN CLUTTER
RANGE: 4600' FOR STUDY)

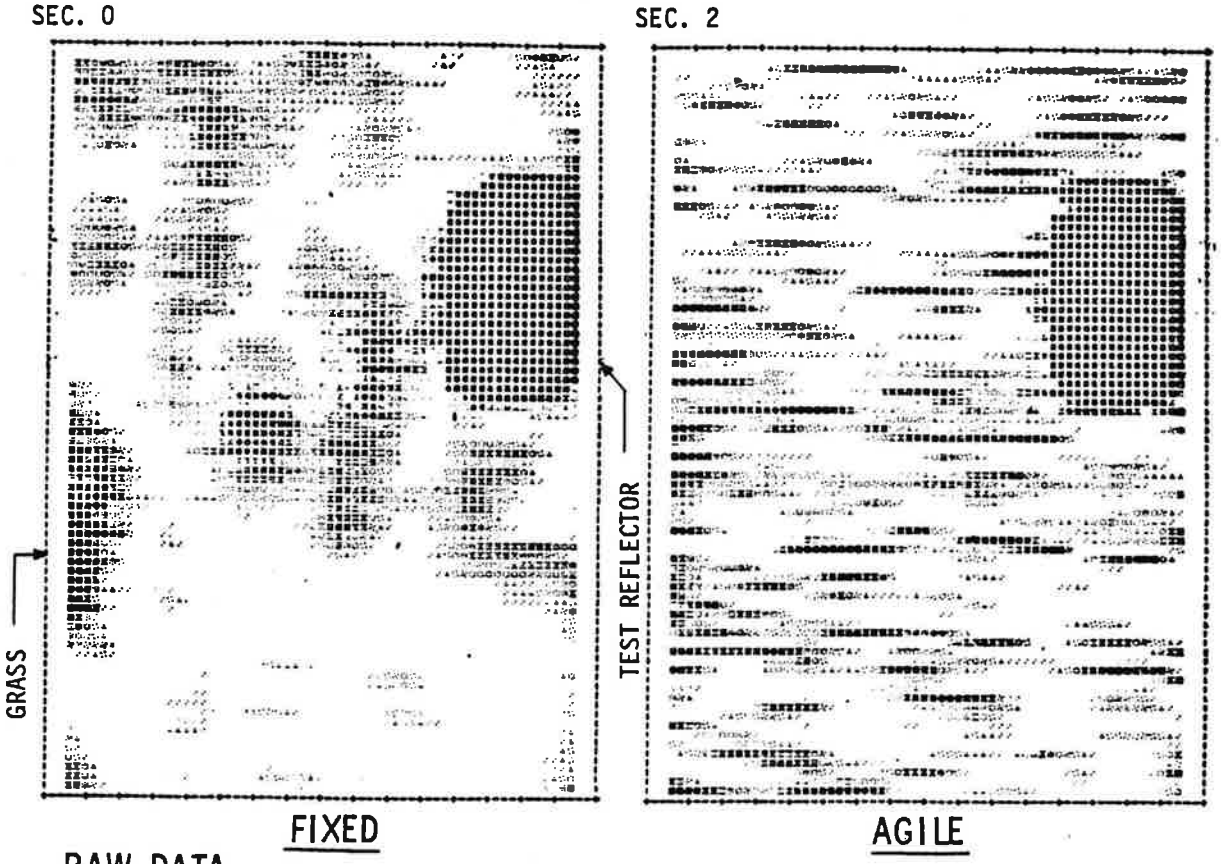

RAW DATA

(SHOWS HOW FREQUENCY AGILITY BREAKS UP 'CLUMPS' OF RAIN RETURNS THAT COULD BE MISTAKEN FOR SMALL TARGETS)

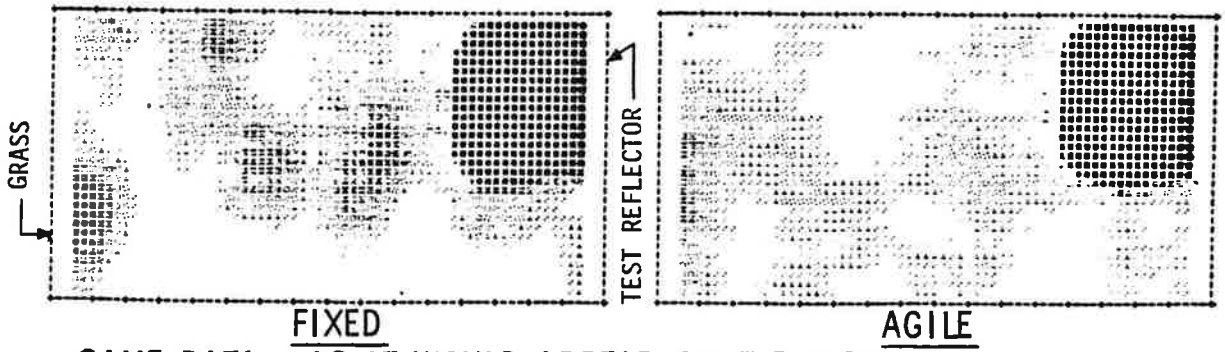

SAME DATA - AS IT WOULD APPEAR ON THE DISPLAY

(SHOWS HOW FREQUENCY AGILITY CAN TRANSFORM STRONGER 'CLUMPS' OF RAIN RETURNS INTO A VERY UNIFORM 'HAZE' THAT WOULD NOT BE MISTAKEN FOR A SMALL TARGET)

FIGURE 5.4-8. PERFORMANCE OF FREQUENCY AGILITY IN RAIN

targets. For frequency agility no two adjacent pulses have strong rain clutter returns, exactly as expected!

The operational benefit from frequency agility is derived from the integration of several radar pulses that occurs on the display. This intensifies the 'false targets' produced by fixed frequency in rain and averages the scattered returns from frequency agility into a light 'mist', the bottom pair of illustrations in Figure 5.4-8 and the middle illustration in Figure 5.5-1 clearly show this effect.

5.5 ADAPTIVE STC AND THRESHOLDING

A feature was designed into the ASDE-3 radar via the Display Enhancement Unit that would allow the receiver STC curve to be adjusted, in real time, to counteract the effects of rain attenuation. This was to be done in up to eight separate azimuth regions and two range regions to allow for spatial variation in attenuation. This feature is referred to as 'adaptive STC' or 'rain gain'.

It was not possible to test this feature due to developmental difficulties experienced. In TSC's judgment these difficulties do not inply that adaptive STC is at all impractical to implement.

Due the wide dynamic range of the receiver, it has been possible to examine the effect and benefit of adaptive STC on ASDE target detection performance. This was done by off-line processing which altered the thresholds for 'displaying' the data.

Figure 5.5-1 illustrates the kind of benefit adaptive STC can provide, (and simultaneously compares frequency-agile with fixed-frequency operation).

The top illustration in Figure 5.5-1 shows a sequence of six radar scans, processed the way the display would 'normally' present the data, that is, no adaptive STC, no threshold. The scans are two seconds apart and alternate between frequency

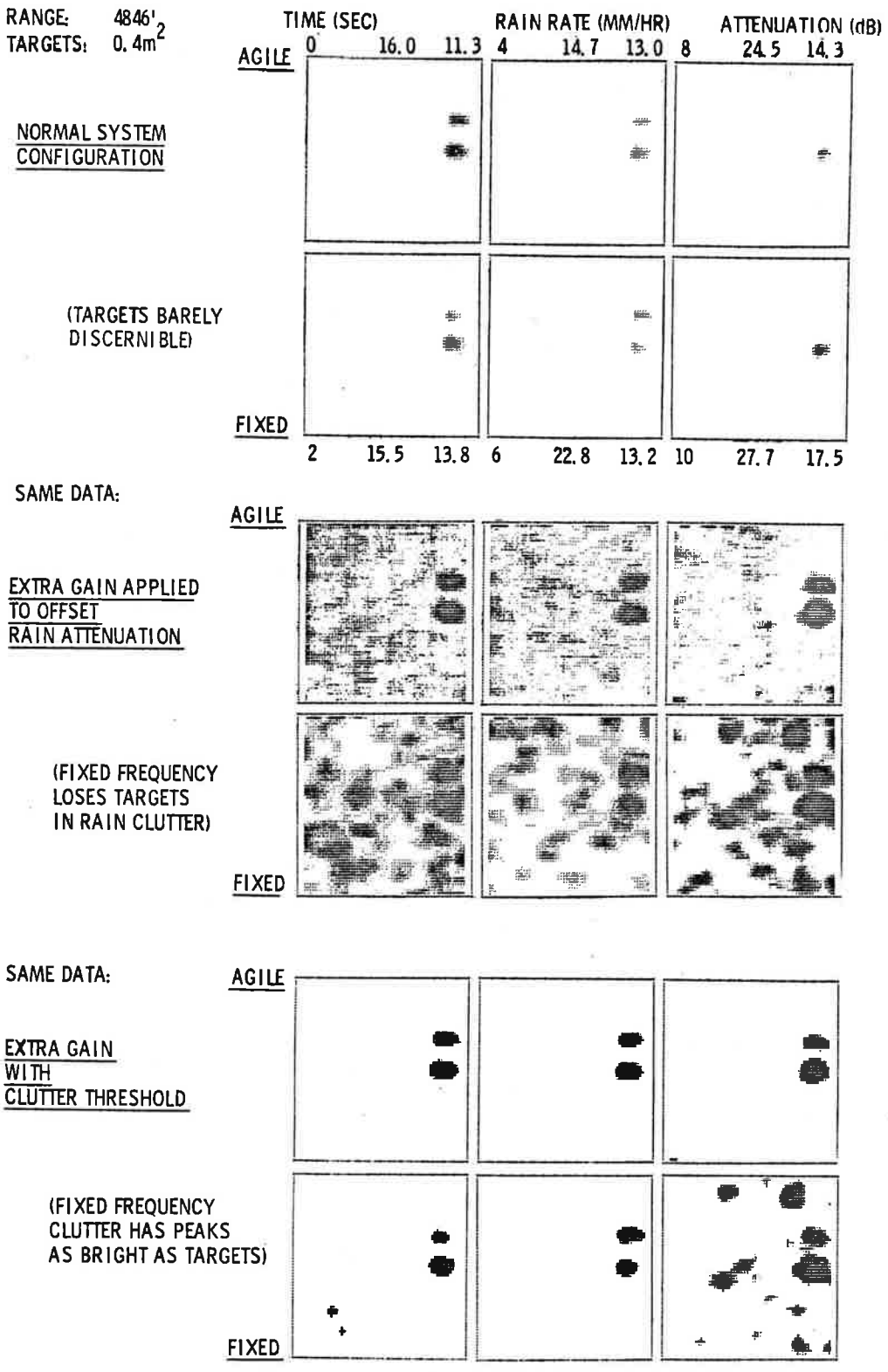

FIGURE 5.5-1. ILLUSTRATION OF FREQUENCY AGILITY BENEFITS IN HEAVY RAIN

agile (top row) and fixed frequency (bottom row). There are two very small test reflectors in the 'window'. As the attenuation increases, the targets go from being light to faint and one disappears altogether.

The middle illustration in Figure 5.5-1 shows the same data as the top illustration, but it is processed to appear the way the display would look with adaptive STC only. Here the targets are restored to being bright but the rain clutter now becomes visible because it, along with the targets, has been amplified above the display threshold. The benefit of frequency agility is clearly evident in this illustration (top row). Frequency agility transforms the rain clutter returns from bright 'clumps and blobs' among which the targets become lost to a uniform 'mist' through which the targets are readily detectable.

Thresholding to Remove Clutter

If an additional threshold, higher than the mean clutter return, but below the smallest target return is applied to the data in addition to using adaptive STC, the target detection and the display appearance are greatly improved. The bottom illustration in Figure 5.5-1 shows the effect on the display appearance, (of adding this threshold to the same data). The targets are now restored to clear weather brightness and rain clutter is dramatically reduced. Again the benefit of frequency agility shows, in that in this case, thresholding can remove practically all rain clutter because frequency agility has smoothed the clutter returns. The clutter returns for fixed frequency have peaks that are as bright as the targets and thus cannot be removed by thresholding.

The idea of applying a clutter threshold to ASDE data is not new. The problem has been in obtaining a reliable measure of the clutter to set the threshold. Sampling the returns on a runway area is not acceptable because an aircraft or other target might cause an erroneous, high reading. Paving special test pads in 16 to 32 areas of the field (each approximately

150 feet square) would be prohibitively expensive.

For ASDE-3, however, it was observed that for low to moderate rainfall the clutter returns are so far below the small target returns that no threshold is required. A threshold is called for when the rain becomes heavy, as in Figure 5.5-1, where the rate varies between 16 and 28 mm/hr. The key is that, for rainfall rates of this magnitude, the attenuation also becomes severe (thus the need for adaptive STC). When the attenuation becomes severe, returns from grass areas on the field become predominated by rain clutter and thus can be used to measure rain clutter power, and to control the threshold. When the rainfall rate is lower, the attenuation is less, and the grass returns predominate, but the clutter return is low so no threshold is used.

The implementation of this technique has been investigated and found to be feasible and relatively inexpensive. The threshold implementation would be similar to adaptive STC and if systematically designed could use duplicate circuitry for storage, calculations, and readout of thresholds.

5.6 RADAR SYSTEM PERFORMANCE MODEL

An objective of the system testing was to verify the detection performance of the ASDE in rainfall predicted by theory. The results of the reduction and analysis of data collected during a severe rainstorm on April 9, 1980 are presented in Section 5.4. The theoretical curves applied to the data shown in Figures 5.4-1, 5.4-2 and 5.4-3 show a good correspondence between theory and data in the mean value sense, with a considerable scatter about the theoretical.

5.6.1 Performance Model Description

The performance model used to produce the theoretical single-pulse (i.e., non-integrated) signal to noise-plus-clutter predicted for the April 9 rainstorm is described in Table 5.6-1.

TABLE 5.6-1. ASDE PERFORMANCE MODEL

1. SIGNAL POWER RECEIVED

$$P_{signal} = \frac{P_t \lambda^2 L L_r G^2 (\Theta) \sigma}{(4\pi)^3 r^4}$$

where:

P_t	=	Transmitted power (peak)
P_{signal}	=	Power at receiver input
λ	=	Wavelength
L_r	=	Total rainfall attenuation (2 way) r $(0.1665\ R^{1.14})$ in dB where R = rainfall rate in mm/hr, r=slant range in nm*
L	=	System Losses
$G(\Theta)$	=	One way elevation power pattern
σ	=	Radar cross-section
r	=	Slant range

*Air Force Cambridge Research Labs, Handbook of Geophysics, page 9-15.

TABLE 5.6-1. ASDE PERFORMANCE MODEL (CONT'D)

2. RAIN BACKSCATTER POWER RECEIVED

$$P_{clutter} = \underbrace{\left[\frac{P_t \lambda^2 L_r L}{(4\pi)^3 r^4}\right]}_{\text{as described for signal power case}} \frac{c\tau n r^2}{2} \int L_p G^2(\theta,\phi)\, d\theta d\phi$$

$\frac{C\tau}{2}$ = Clutter volume depth (pulse resolution)

c = Speed of light 3×10^8 m/s

τ = Pulse width 36 ns

n = Rainfall backscatter coefficient

$$= \frac{\pi 5}{\lambda 4} (0.93) (200R^{1.6})^* 10^{-18*}$$

where R = rainfall rate in mm/hr, λ in meters, and n is in units of 1/m

$L_p(\Theta)$ = Cancellation Ratio (Function of Elevation Angle)

$G(\Theta,\phi)$ = One way power pattern (azimuth and elevation)

*AFCRL Handbook of Geophysics, page 9-9.

TABLE 5.6-1. ASDE PERFORMANCE MODEL (CONT'D)

3. RECEIVER NOISE POWER

Noise Power at Input of r.f. Amplifier = k TBNF

where:

k	=	Boltzman's constant
T	=	Temperature (290 degrees Kelvin)
B	=	Receiver Bandwidth, MHz
NF	=	Receiver noise figure at input to r.f. amplifier; includes effects of following stages

4. SINGLE PULSE SIGNAL TO NOISE-PLUS-CLUTTER

$$S/(N+C) = \frac{P_{signal}}{P_{clutter} + k\ TBNF}$$

The parameters used in the model listed in Table 5.6-2 are those values measured at FAATC. An integrated cancellation ratio of 10 is used, lower than the value measured for the antenna rotodome on the free space range. This is done to simulate the effect of the multiple clutter volume. Figure 5.6-1 shows a plot of the single pulse S/(N+C) predicted for the ASDE at FAATC for the $3m^2$ specified target. The specification limits of 13 dB S/(N+C) in 16 mm/hr rainfall are shown. Ample performance margin in rainfall exists for the system as installed, even with the high loss for the WR-62 waveguide run. This is consistent with our ability to observe the small metal brackets (RCS estimated to be $0.4m^2$) in very heavy rain at Pads 2 and 3 as seen in the April 9 rain data.

5.6.2 Performance Predicted for the Specified System and Target $3m^2$

Figures 5.6-2 and 3 show the S/(N+C) predicted for the ASDE-3 for the recommended specification parameter values. These values are listed in Table 5.6-3. The first plot shows the performance for a 200 ft. tower, representing the tallest control towers now in the field (except Logan). Ample margin to meet the specification is available at 18,000 ft., as shown. Figure 5.6-3 shows performance predicted for the 300 ft tower. Performance margin begins to diminish at close ranges where the targets in the shaped- beam region are competing with rain clutter heavily gain-weighted by the elevation boresight region.

5.6.3 Frequency Agility Benefits for Target Detection in Railfall

The 5 to 6 dB benefit in rainfall penetration performance for frequency agility seen in the review of the data (See Section 5.4.2) does not match theoretical predictions for the integration of several pulses. There is no reason to believe that the theoretical premise of frequency agility benefits is not valid. Certainly there is a substantial effect of frequency agility seen in the rain data. It should be pointed out,

TABLE 5.6-2. ASDE-3 SYSTEM PARAMETERS USED IN S/(N+C) MODEL

P_t	+ 68 dBm (measured at output of circulator)
L	13.5 dB (Measured Data, to input of pedestal - includes xmit and receive path losses)
λ	0.06152 Ft (16.0 GHz)
σ	0.4 M^2, $3M^2$
G_o	45 dBic (ref. input to pedestal)
$G(\theta)$	Teledyne Range - measured elevation pattern.
ϕ	0.27°
L_P	10dB
τ	36 ns
NF	6.5 dB
B	50 MHz

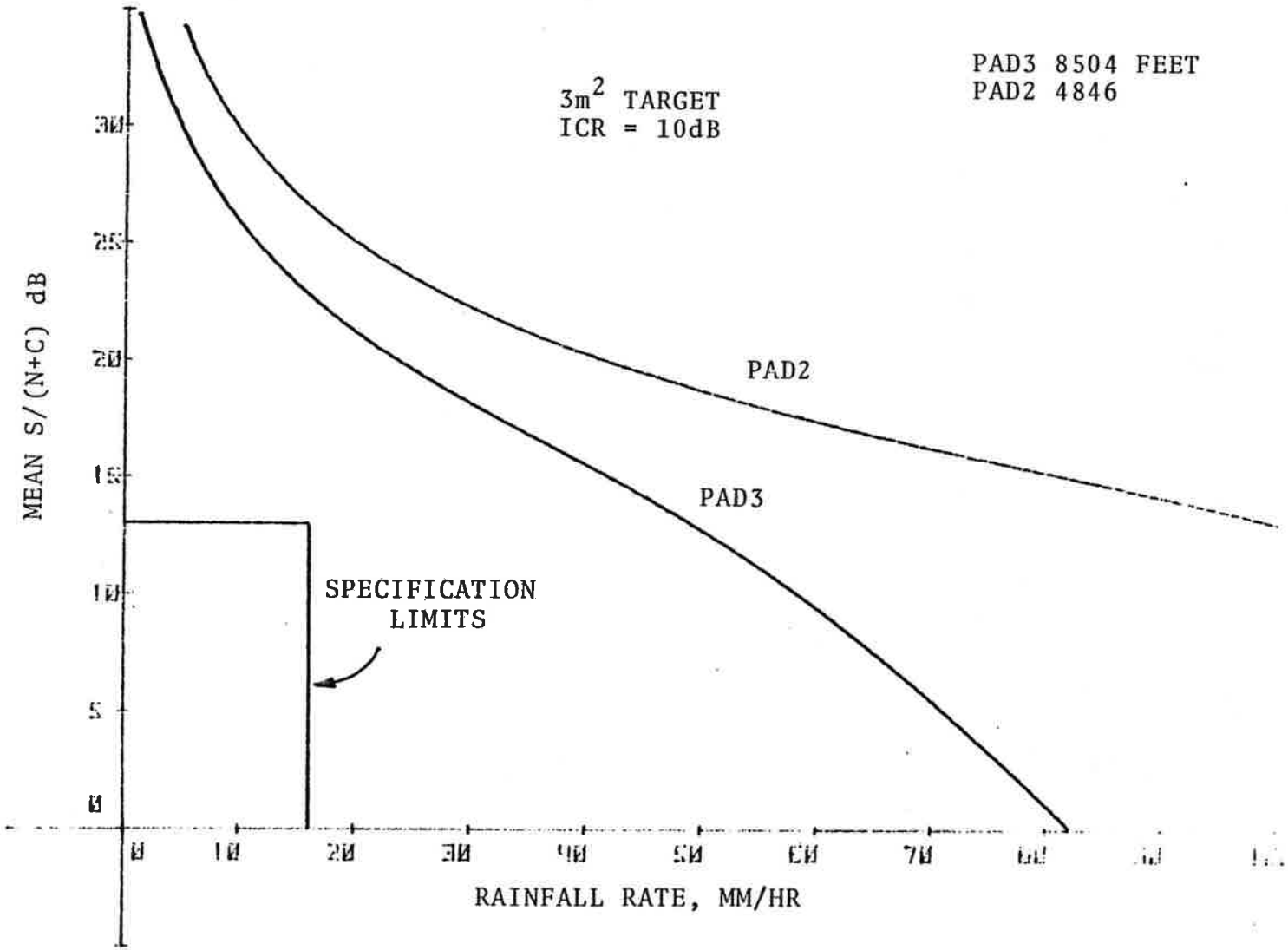

FIGURE 5.6-1. MEAN S/(N+C) FOR THE ASDE-3 INSTALLED AT FAATC

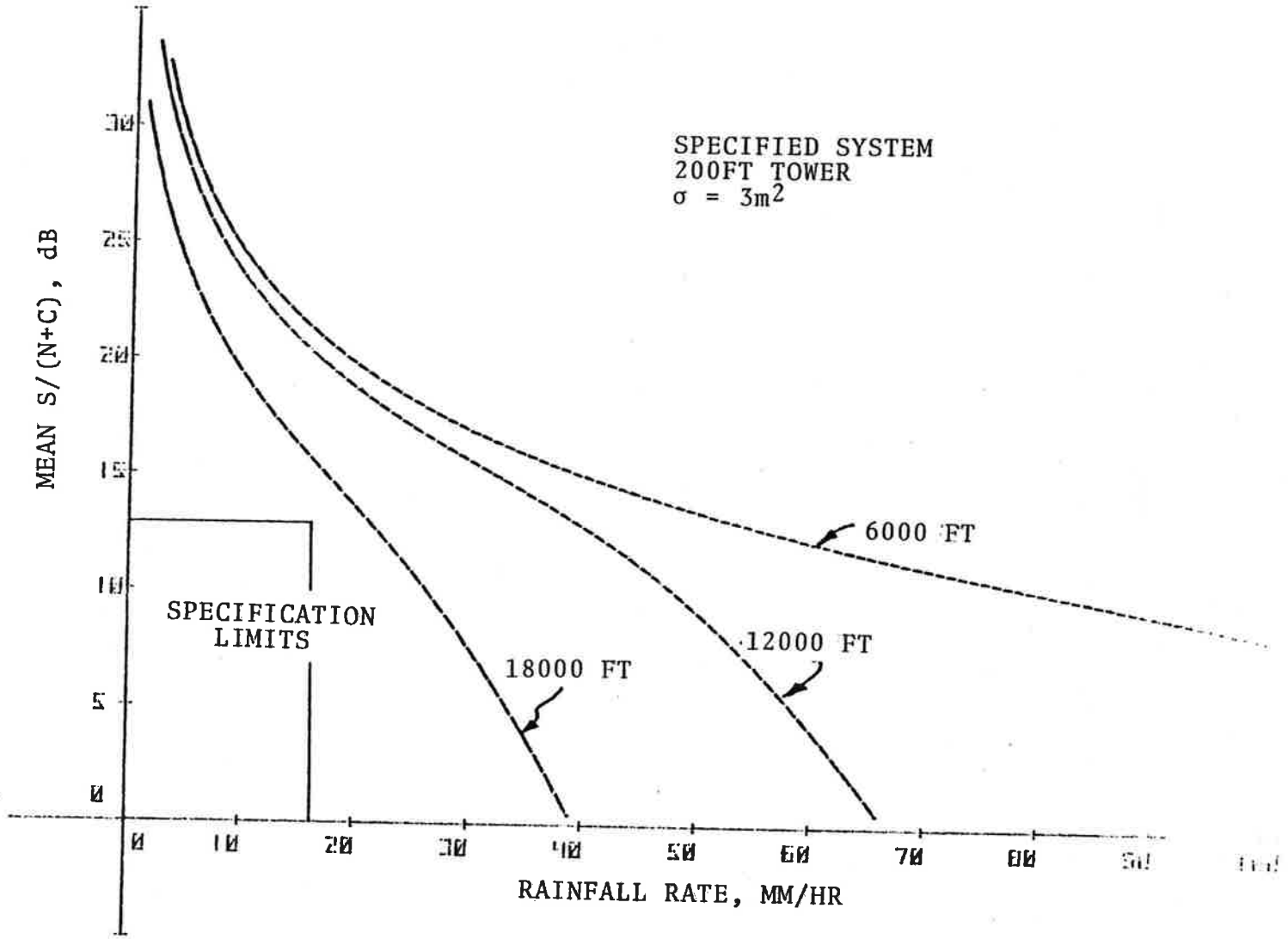

FIGURE 5.6-2. MEAN S/(N+C) FOR THE SPECIFIED SYSTEM, 200-FOOT TOWER

TABLE 5.6-3. ASDE-3 SPECIFICATION PARAMETERS

P_t	+70 dBM
L	6.7 dB (Low loss rectangular waveguide 100 ft run)
G_o	45 dBic (ref. input to pedestal)
L_p	10 dB
τ	36 ns
NF	6.0 dB
B	40 MHz

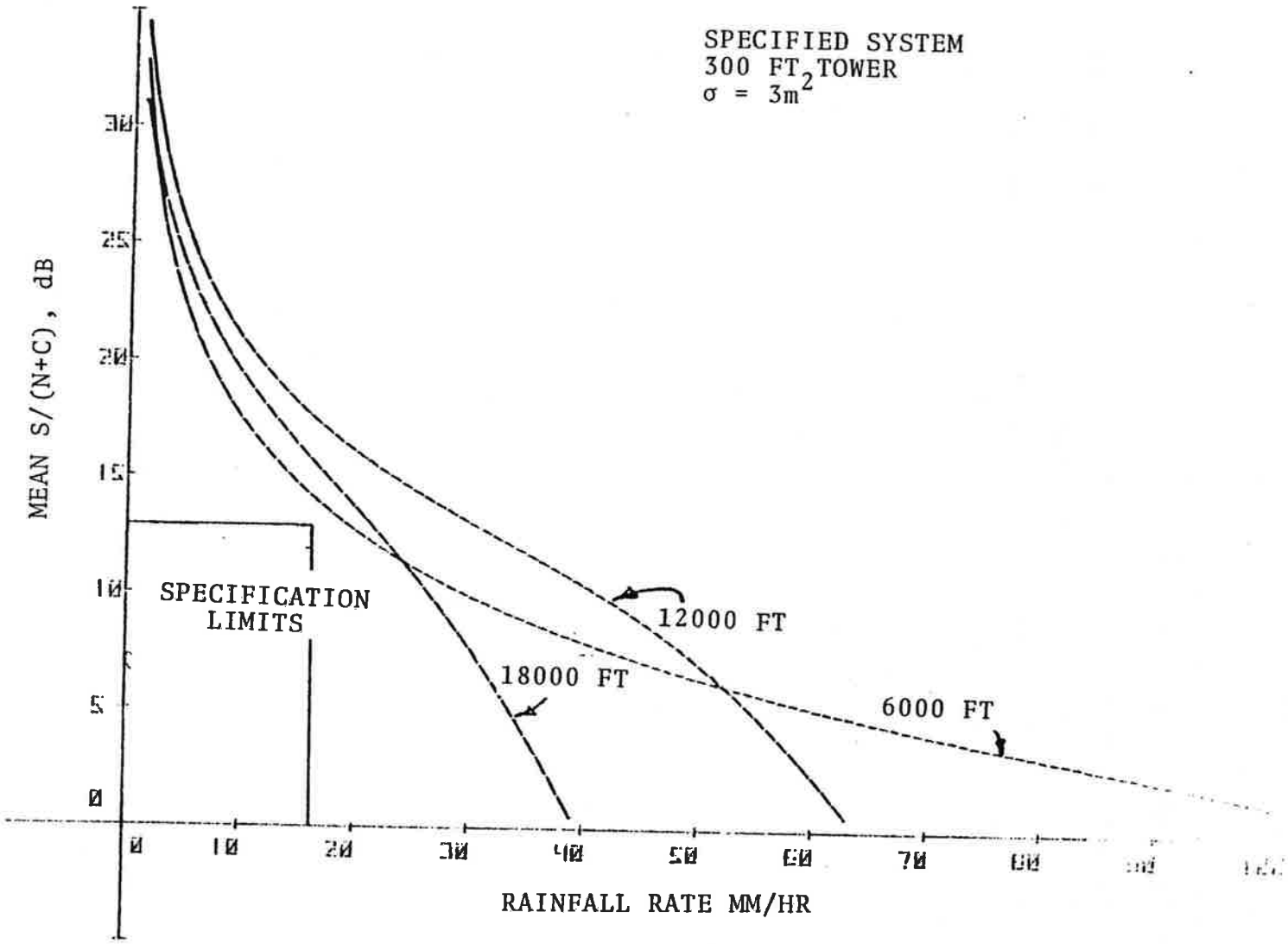

FIGURE 5.6-3. MEAN S/(N+C) FOR THE SPECIFIED SYSTEM: 300-FOOT TOWER

however, that the improvement offered by frequency agility is not uniformly applicable across the range of rainfall rates expected in actual operation. The improvement of frequency agility for multiple pulse integration is only valid when the S/(N+C) ratio is dominated by rainclutter, i.e., mean clutter is substantially above receiver noise.

Figure 5.6-4 (theoretical mean return power for backscatter from rainfall for the 200 ft tower case with a -92 dBm (KTBF) receiver noise level) shows that at 18,000 ft the mean clutter is substantially above receiver noise only in a limited region of rainfall rates around 10 mm/hr. The shape of the curves is caused by two countering effects!

1. For low rainfall rates, backscatter is low, resulting in low rain clutter return power.
2. For high rainfall rates, the backscattering cross section is high, but the net rain clutter return power is low because rain path attenuation effects predominante.

It can be seen in Figure 5.6-4 that in the central peak region the two opposing effects (i.e., increasing backscatter and increasing attenuation) are at a standoff, producing a maximum. For ranges within 2 nmi, however, rain clutter power predominates for rain rates between 5 and 30 mm/hr. Here the decorrelation benefits of pulse-to-pulse agility apply for multiple pulse integration.

Figure 5.6-5 illustrates (in the case shown for 16 mm/hr.) that rain attenuation increases with range, and rain backscatter decreases with range.

The ASDE-3 performance specification requires detection of a 3 m^2 non-fluctuating target (Swerling Case 0) at 18,000 ft in range in a 16 mm/hr rainfall for a single pulse S/(N+C) of 13 db. In reality, actual targets measured at the field test site were seen to fluctuate highly from scan-to-scan. The small automobile discussed in Section 5.2.1 was found to be a fluctuat-

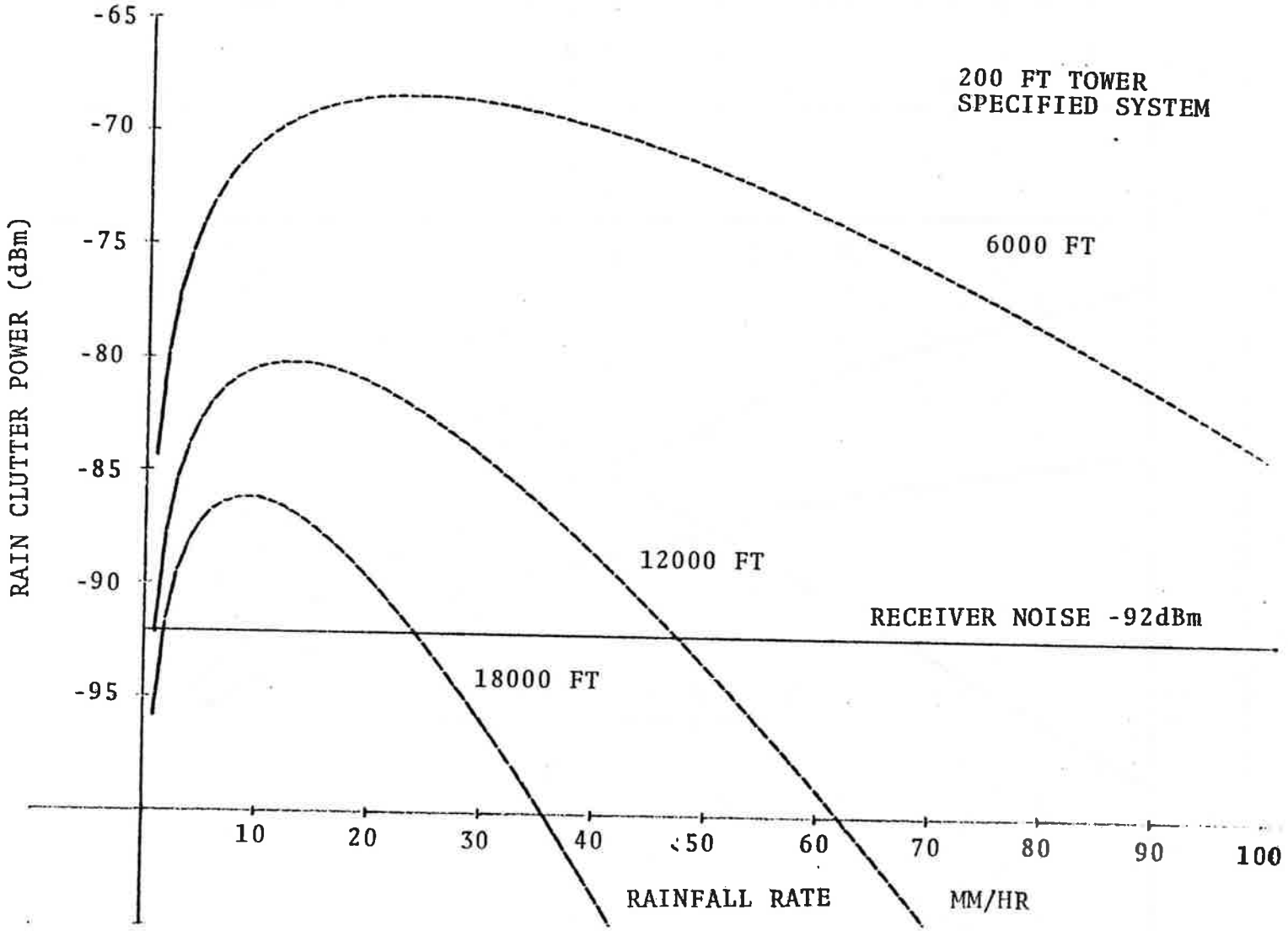

FIGURE 5.6-4. MEAN RAIN CLUTTER POWER FOR THE 200-FOOT TOWER SPECIFIED SYSTEM

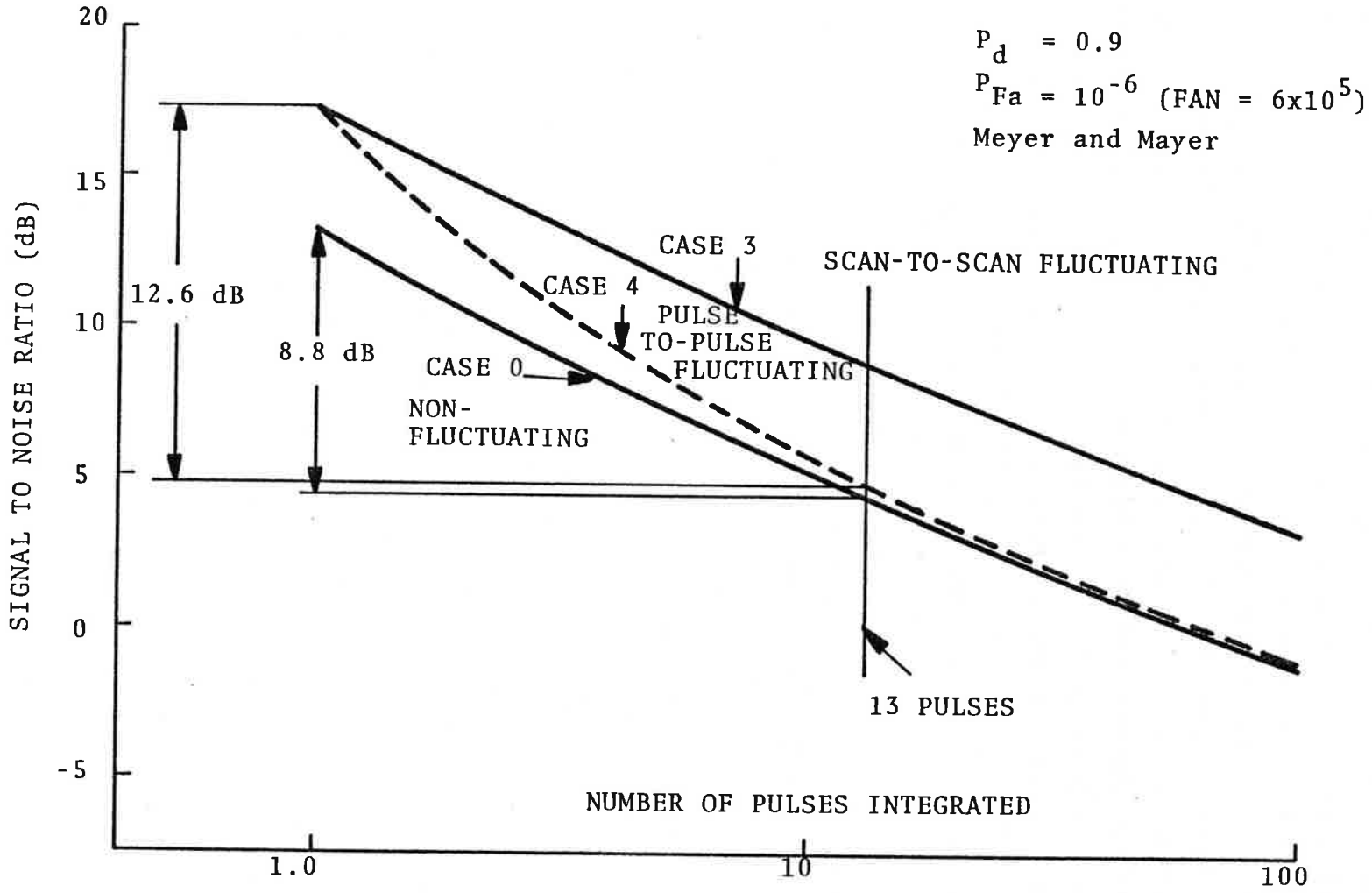

FIGURE 5.6-7. DETECTION PERFORMANCE FOR FLUCTUATING TARGET IN RAIN CLUTTER

highly variable nature of the rain in the April 9, 1980 rainstorm.

2. The specified system should be able to perform in 16 mm/hr rainfall out to 18,000 ft for a $3m^2$, non-fluctuating target, for either agile or fixed frequency operation. For fixed frequency operation the system performance is significantly impaired at the specified rainfall rate of 16 mm/hr for the fluctuating small target,such as an automobile or small aircraft.

3. Frequency agility is predicted to allow the system to perform out to 12,000 ft for a fluctuating small vehicle target (0.3 m^2 estimated at the 90% point of the distribution) in 16 mm/hr rainfall based on extrapolations of the data taken at FAATC. A 9 dB net benefit for frequency agility is based on a combination of rain penetration and fluctuating target conversion benefits.